Neural Mechanisms of Visual Context Processing in Healthy Adults and those with Schizophrenia

A THESIS SUBMITTED TO THE FACULTY OF
UNIVERSITY OF MINNESOTA
BY

Michael-Paul Schallmo

IN PARTIAL FULFILLMENT OF THE REQUIREMENTS
FOR THE DEGREE OF
DOCTOR OF PHILOSOPHY

Cheryl A. Olman, Advisor

December 2014

Acknowledgements

I would like to thank all of the professors and teachers who have guided me through my PhD and shepherded my work, in particular Scott Sponheim and my advisor Cheryl Olman. Thanks also to all of my colleagues and classmates, including Cheng Qiu and Damien Mannion. Andrea Grant and Phil Burton also deserve special mention for their technical assistance, especially with the Flankers project. Members of the Sponheim lab who assisted with data collection and subject recruitment also deserve recognition. Finally, I want to express my gratitude to everyone who volunteered their time and energy as part of this research.

This work was supported by the National Institute of Health (R21 NS075525 to CAO, T32 GM0847, P30 EY011374, P30 NS076408, P41 EB015894, S10 RR026783), the National Science Foundation (GRF 00006595 to MPS), the University of Minnesota Graduate School (Doctoral Dissertation Fellowship to MPS), the Veterans Health Administration (CSMRF I01CX000227-01 to SRS), and the WM KECK Foundation.

Dedication

This thesis is dedicated to everyone I love, and all those who supported or inspired me. First and foremost, to my wife Karin, who fills my life with joy. To my parents Mike and Kathy, and my sister Kristin, for always believing in me. To my friends for making me laugh. To all the family who have done so much. To my dog Luna, for being a lot of fun. To Veronica and Warren Schallmo, Elston and Pauline Gaurin, TP and Dawn Cockrel, and Mike Burton, who live on in my heart. To all those impacted by mental illness.

Abstract

The brain's response to a visual stimulus depends in part on the context in which it appears. For example, objects appearing within similar-looking backgrounds tend to evoke smaller neural responses than those seen in isolation. While it is known that schizophrenia (SZ) may reduce visual context effects, the neural mechanisms involved are not fully understood. This dissertation uses functional magnetic resonance imaging (fMRI) and visual behavioral tasks to examine the role of context during normal visual processing, and how context processing is affected by SZ.

Chapter 1 provides an overview of the forms of contextual modulation that will be addressed later, and their impairment in SZ. Chapter 2 describes a series of five experiments probing how factors such as stimulus geometry, presentation timing, and attention affect the fMRI response to small groups of visual stimuli. In primary visual cortex, the relative strength of contextual modulation was found to increase when subjects directed their attention away from the stimuli. Further, fMRI responses to parallel center and surrounding stimuli did not show the predicted sensitivity to center contrast.

In Chapters 3 and 4, the effect of spatial context during early visual processing in SZ patients was assessed using behavioral measures. Surround suppression of perceived contrast was examined in Chapter 3 among SZ patients and their unaffected relatives, as well as subjects with bipolar affective disorder (BP), relatives of BP subjects, and healthy controls. Weaker surround suppression was observed in SZ versus control subjects, while BP patients showed an intermediate deficit. These deficits did not depend on the

configuration of surrounding stimuli. Normal performance was observed among relatives of SZ and BP subjects, indicating deficits in surround suppression were not associated with a genetic risk for these disorders. Chapter 4 examined how SZ impairs the ability to detect visual contours in cluttered backgrounds. Contours were presented in more- or less-similar backgrounds, in order to assess contextual modulation. While SZ patients performed worse than healthy controls or SZ relatives when detecting contours, performance in SZ was less influenced by background context.

These experiments were designed to explore the neural basis of visual context processing in healthy adults, and to help uncover how SZ impairs these processes. The large body of research into the neurophysiology of human vision provides powerful tools with which to study how SZ may disrupt neural processing. Studying visual context processing may ultimately help to uncover computational principles conserved across many neural systems, and aid in identifying new targets for the treatment of mental disorders.

Table of Contents

List of Tables

List of Figures

List of Equations

Chapter 1 :

Contextual Modulation of Early Visual Processing

One of the major problems in vision research is to understand how neurons process interactions between visual stimuli. For example, how does the brain's response to seeing a zebra alone on the savannah differ from the response to the same zebra seen within a herd? The neural response to a visual stimulus such as an object depends on the specific context (e.g., background) in which the object appears. Typically, neurons in visual cortex respond more strongly to a stimulus that stands out from the background than one that is similar to the surrounding context (e.g., camouflage; Cavanaugh et al., 2002). However, in patients with schizophrenia this modulation is diminished, reflecting an abnormally weak influence of context during visual processing (Butler et al., 2008). This abnormality may be related to the visual illusions and hallucinations experienced by some patients with this disorder. However, until we understand the neural processes underlying context effects in vision, we will not know how schizophrenia impairs these processes.

Context Processing in Healthy Vision

The pioneering work of Hubel and Wiesel (1962, 1968) showed that for neurons in primary visual cortex (V1), visual stimuli such as edges or line segments evoke a response when presented within the spatial region of the classical receptive field (cRF),

while those outside do not. They also found that in some cases, increasing the stimulus size beyond the cRF led to a reduced response. This work led to the study of what has become known as the extra-classical receptive field (ecRF), a region outside of the cRF that does not evoke neural responses when stimulated alone, but is capable of modulating the response to stimuli presented simultaneously within the cRF. Typically, ecRF stimulation reduces responses compared to cRF stimulation alone, an effect known as surround suppression. In agreement with Hubel and Wiesel, size-tuning experiments have shown that stimuli filling the cRF evoke maximal response amplitudes, while larger stimuli that extend into the ecRF tend to yield smaller responses (DeAngelis et al., 1994; Angelucci et al., 2002). Results from psychophysical (Cannon and Fullenkamp, 1991) and functional imaging (Nurminen et al., 2009) size-tuning experiments in humans also show surround suppression in response to center and surrounding stimuli designed to match the spatial profile of V1 cRFs and ecRFs, respectively. Thus, larger stimuli that evoke greater ecRF stimulation tend to produce stronger surround suppression across experimental paradigms.

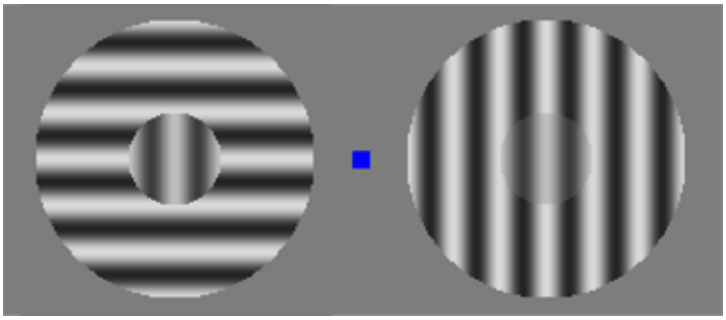

Figure 1-1. An example of orientation-dependent surround suppression.
When focusing on the square in the middle, the center of the left stimulus (with an orthogonal surround) is perceived to have relatively high contrast. The contrast of the physically identical region at the same position on the right (with a parallel surround) appears much lower.

The magnitude of surround suppression also depends on the similarity of visual stimuli appearing within the center and surrounding regions. Stronger suppression is typically seen when surrounding features match those in the center (e.g., parallel orientation; Figure 1-1), as shown in electrophysiological (DeAngelis et al., 1994; Cavanaugh et al., 2002; Shushruth et al., 2012; Henry et al., 2013), psychophysics (Cannon and Fullenkamp, 1991; Xing and Heeger, 2000; Yu et al., 2001), and fMRI experiments (Williams et al., 2003; Pihlaja et al., 2008; McDonald et al., 2010). Relative contrast is somewhat of an exception to this similarity-suppression rule; higher-contrast surrounds often evoke stronger suppression than is seen with equal center and surround contrast (Yu et al., 2001; Cavanaugh et al., 2002; Henry et al., 2013). Matching spatial phase can also produce stronger suppression (Yu et al., 2001; Williams et al., 2003; Xu et al., 2005), but this appears to depend on the proximity of surrounding stimuli, as the addition of a small gap (< 0.5°) is sufficient to disrupt phase sensitivity (Yu et al., 2001). Surround proximity can additionally affect the overall magnitude and sign of modulation; in some cases surrounds that are widely separated from the center (> 7°) are capable of facilitating responses (Ichida et al., 2007).

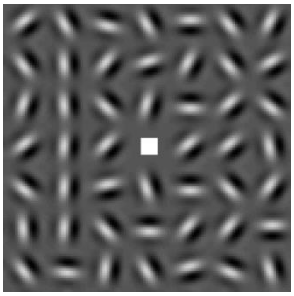

Figure 1-2. Contour integration example.
Collinear Gabor stimuli (5 vertically aligned, 2 rows left of the center fixation square) form the percept of a coherent line segment or contour within the cluttered background.

In another form of spatial context modulation, response enhancement is often observed when oriented visual stimuli may be grouped into a coherent line or contour (Loffler, 2008). Strong grouping is typically observed when the orientation of each segment matches the global stimulus orientation. When aligned along the ends of a central target, flanking line segments can increase neural responses (Polat et al., 1998; Ito and Gilbert, 1999; Chen et al., 2001) and perceptual detection / discrimination (Freeman et al., 2001; Zenger-Landolt and Koch, 2001; Freeman et al., 2003), an effect known as collinear facilitation. For collinear stimuli presented within a noisy or cluttered background (Figure 1-2), contour integration typically enhances detection / discrimination (Field et al., 1993; Bonneh and Sagi, 1998; Li and Gilbert, 2002; Dakin and Baruch, 2009; Schumacher et al., 2011b) and strengthens neural responses measured via electrophysiology (Bauer and Heinze, 2002; Li et al., 2006; Li et al., 2008a) or imaging (Altmann et al., 2003; Gilad et al., 2013). Like surround suppression, the strength of collinear facilitation and contour integration also depends on factors such as element spacing and relative contrast (Field et al., 1993; Polat et al., 1998). It has been proposed that surround suppression and collinear facilitation may depend on some of the same neural circuitry (Angelucci and Bullier, 2003). Electrophysiology (Polat et al., 1998; Walker et al., 1999; Gilbert et al., 2000) and computational modeling (Zeng et al., 2011) suggest that stimuli which activate ecRF “end” regions (along the axis of a neuron’s preferred orientation) may facilitate or suppress cRF responses depending on the relative center-surround configuration, while “side” regions (tangential to the preferred orientation) are more likely to evoke suppression. This agrees with recent

psychophysical work (Dakin and Baruch, 2009; Schumacher et al., 2011b) examining how contour integration and surround suppression both depend on factors such as the relative orientation of contour (end-aligned) and background (side-flanking) elements.

The neural mechanisms underlying spatial context processing are not fully understood. As surround modulation is orientation selective (i.e., parallel surrounds typically evoke stronger suppression than those orthogonal to the center), it has been suggested that these effects originate within early visual cortex, where strong orientation selectivity is observed (DeAngelis et al., 1994). Anatomical (Angelucci et al., 2002; Angelucci and Bullier, 2003; Angelucci and Bressloff, 2006) and functional (DeAngelis et al., 1994; Bair et al., 2003; Ozeki et al., 2004; Roinishvili et al., 2008; Ozeki et al., 2009; Shushruth et al., 2012; Nassi et al., 2013) studies have suggested that contextual modulation in V1 may depend on a combination of feed-forward modulation from the lateral geniculate nucleus (LGN), horizontal connections between distal regions in V1, and feedback from higher visual areas (e.g., V2 and MT). In particular, many electrophysiological (Bair et al., 2003; Webb et al., 2005) and behavioral studies (Cannon and Fullenkamp, 1991; Paffen et al., 2005; Cai et al., 2008) have suggested multiple neural mechanisms underlie surround suppression, including separate broadly and sharply orientation tuned components. The role of particular neurotransmitters in contextual modulation is also not clear; while some studies point to inhibition by γ-amino butyric acid (GABA; Haider et al., 2010; Ma et al., 2010; Yoon et al., 2010; Adesnik et al., 2012; Atallah et al., 2012; Nienborg et al., 2013), others suggest excitation by glutamate (and the withdrawal thereof) may play a larger role in contextual facilitation or suppression

(Crook et al., 2002; Ozeki et al., 2004; Ozeki et al., 2009; Shushruth et al., 2012). New tools such as optogenetics (Adesnik et al., 2012; Atallah et al., 2012; Nienborg et al., 2013) may further clarify the precise role of different neurotransmitters and circuits during spatial context modulation in early visual cortex.

Impaired Context Processing in Schizophrenia

In addition to abnormal visual percepts (hallucinations, illusions) experienced by some patients with schizophrenia (SZ), a number of more subtle visual processing abnormalities have been observed in this disorder, including weaker modulation by spatial context. As visual neuroscience is relatively well-studied, understanding how SZ affects early visual processing offers great potential for elucidating the neural basis of this disorder (Butler et al., 2008; Phillips and Silverstein, 2013; Yoon et al., 2013; Notredame et al., 2014). In particular, impairments in visual gain control and integration (i.e., surround suppression and contour perception) have been highlighted among patients with SZ (Butler et al., 2008; Phillips and Silverstein, 2013). Paradigms designed to measure these processes in SZ have been noted for their potential utility in clinical trials (Gold et al., 2012). However, the precise neural deficits that give rise to such visual abnormalities are not clear. A better understanding of how spatial context processing is impaired in SZ may therefore improve diagnosis of this disorder, and help to identify particular neural abnormalities for which better treatments may be developed.

Weaker surround suppression during contrast perception has been observed among patients with SZ by multiple groups using different paradigms (Dakin et al., 2005; Tadin et al., 2006; Yoon et al., 2009; Barch et al., 2012; Robol et al., 2013; Tibber et al.,

2013; Yang et al., 2013), including a study using functional MRI in V1 (Seymour et al., 2013). Another study using magnetic resonance spectroscopy found lower concentrations of GABA in early visual cortex were associated with diminished surround suppression across a group of healthy subjects and those with SZ (Yoon et al., 2010). Abnormally weak surround suppression may be specific to contrast perception; relatively normal contextual modulation has been reported for other early visual percepts such as luminance (Tibber et al., 2013; Yang et al., 2013). Some have suggested that deficient surround suppression in SZ may depend on abnormal contextual modulation of neural activity within V1 (Yoon et al., 2009; Seymour et al., 2013; Yang et al., 2013). However, to date it is not known whether this deficit may be attributed to a more specific neural mechanism in early visual cortex (e.g., horizontal connections within V1, versus feedback from higher visual areas).

Impaired contour perception has also been consistently reported in SZ (Silverstein et al., 2000; Parnas et al., 2001; Uhlhaas et al., 2005; Silverstein et al., 2006b; Uhlhaas et al., 2006; Keane et al., 2012; Butler et al., 2013). A study using fMRI has suggested that poorer contour integration may depend on weaker activation in early / intermediate visual areas V2, V3, and V4 (Silverstein et al., 2009). Behavioral and EEG studies of illusory contour perception have also reported deficits in SZ (Spencer et al., 2003; Spencer et al., 2004; Foxe et al., 2005; Keane et al., 2014), often attributing them to poorer high-level shape representations among patients. In contrast, weaker collinear facilitation among SZ subjects has also been observed (Must et al., 2004; Kéri et al., 2005), suggesting a lower-

level deficit. Thus, while poorer contour perception is well documented in SZ, it is not clear at what stage(s) in the visual processing hierarchy such deficits originate.

Significance

Spatial context processing plays an important role in human behavior by helping to efficiently calculate and encode the salience of visual stimuli. Many spatial context effects including surround suppression can be explained in terms of a normalization model (Heeger, 1992; Carandini and Heeger, 2012). In normalization, a neuron's response is divided by the summed response of its neighbors, thereby evoking suppression for stimuli filling the ecRF. It has been proposed that normalization may reduce redundancy and increase sensitivity of neural responses across multiple brain systems (e.g., visual, auditory, attentional), thereby making them more efficient.

Both surround suppression and collinear facilitation are believed to play a role in distinguishing objects from backgrounds (figure-ground segregation), by highlighting the neural representations of edges relative to homogenous portions of an image (Hubel and Wiesel, 1968; Polat et al., 1998; Poort et al., 2012; Yoon et al., 2013). Recent studies have found that the strength of surround suppression increases for stimulus conditions which evoke greater perceptual grouping, suggesting a role in global pattern perception (Joo et al., 2012; Joo and Murray, 2013). It has also been suggested that surround suppression may serve to maintain consistent percepts regardless of viewing conditions. For example, the appearance of a low contrast center region within a higher contrast surround is consistent with viewing the center through a medium with imperfect transmittance such as a tinted glass. An empirical interpretation of surround suppression

therefore holds that stimulus configurations consistent with imperfect transmittance evoke stronger suppression than those that are inconsistent (Lotto and Purves, 2001). Finally, studying the neural computations underlying visual context processing may also provide insight into conditions in which these processes are impaired, such as in SZ.

It is not yet clear how early visual processing deficits are related to other problems and symptoms associated with SZ. Deficits in contour perception have been associated with both visual hallucinations (Spencer et al., 2004) and cognitive disorganization (Silverstein et al., 2000; Spencer et al., 2004; Uhlhaas et al., 2006; Butler et al., 2013). It has been proposed that impaired surround suppression and contour perception in SZ may reflect a broader deficit in "context-sensitive gain control" (Phillips and Silverstein, 2013); neural activity across the brain may be less precisely modulated by contextual information. This may impair the ability to form high-level predications about the environment (e.g., concavity versus convexity of a visual stimulus; Dima et al., 2009; Dima et al., 2010; Keane et al., 2013), which could lead to misperceptions, hallucinations, or delusions (Fletcher and Frith, 2009). This framework suggests a common mechanism may underlie impaired visual processing and some of the positive and/or cognitive symptoms observed in SZ. However, little to no association has been found between tasks measuring contour integration, surround suppression, object encoding and working memory, suggesting these cognitive processes are impaired separately in SZ (Gold et al., 2012). Interestingly, similar deficits in visual context processing have also been associated with autism spectrum disorder (Happé, 1996; Walter et al., 2009; Chouinard et al., 2013), raising the question of whether such

impairments may point to neural dysfunction common to multiple disorders. Elucidating the way in which SZ affects visual context modulation may therefore improve our understanding of how this disorder (and perhaps others) can impair neural processing across multiple brain systems.

Chapter 2 :

Examining Contrast Sensitivity in the V1 fMRI Response during Iso-Orientation Surround Suppression

Authors: Michael-Paul Schallmo, Andrea N. Grant, Philip C. Burton, and Cheryl A. Olman

To be submitted to *NeuroImage*

Summary

Functional MRI data are typically interpreted as measurements of average, local neural population activity. However, when a neural population encodes multiple aspects of a stimulus or behavioral state, quantitative inference is difficult. For example, the modulatory effects of stimulus context, attention, or behavioral task can confound interpretation of the local BOLD signal in visual cortex. We conducted five fMRI experiments to understand the contributions of task, timing, and stimulus geometry during visual context processing. The response to small sinusoidal grating patches with different surrounding gratings was measured in human subjects using a 7 Tesla scanner with 1.2 mm isotropic resolution. Target grating patches were presented at 8%, 16% and 32% contrast while manipulating: (1) spatial extent of parallel (strongly suppressive) or orthogonal (weakly suppressive) surrounds, (2) locus of attention, (3) stimulus onset asynchrony between the target and surround, and (4) temporal structure of stimulus

presentation (blocked versus event-related design). In all experiments, the V1 fMRI signal was lower when target stimuli were flanked by parallel versus orthogonal context, as expected. However, only with orthogonal surrounds did we observe the expected contrast sensitivity; parallel condition responses showed little or no increase above baseline with greater target contrast.

Introduction

The relationship between neural activity in primary visual cortex (V1) and the contrast of an individual stimulus is well established. Functional MRI (fMRI) responses in V1 increase with greater stimulus contrast (Boynton et al., 1996; Boynton et al., 1999; Zenger-Landolt and Heeger, 2003; Olman et al., 2004; Schumacher et al., 2011a), and these responses can be predicted based on contrast discrimination psychophysics (Boynton et al., 1999; Zenger-Landolt and Heeger, 2003). However, understanding how V1 also encodes contextual interactions between stimuli has proved more challenging, as the V1 fMRI response does not always reflect the modulation predicted by the spatial configuration of adjacent stimuli (Schumacher and Olman, 2010; Joo et al., 2012).

The current study uses a surround suppression paradigm to examine the ability of fMRI to measure the neural representation of visual contrast, and how these representations are modulated by surrounding context. Surround suppression is a well-studied example of contextual modulation in V1; a neuron's response to a stimulus in its classical receptive field is typically suppressed by simultaneous presentation of surrounding stimuli (DeAngelis et al., 1994; Levitt and Lund, 1997; Walker et al., 1999;

Cavanaugh et al., 2002; Webb et al., 2005; Ichida et al., 2007; Henry et al., 2013; Shushruth et al., 2013). The magnitude and sign of surround modulation depends on feature similarity between center and surround, with more similarity typically evoking greater suppression. Thus, in orientation-dependent surround suppression (ODSS) the response to a grating is suppressed more by parallel than by orthogonal surrounds. Psychophysically, parallel surrounds impair contrast detection and discrimination, and reduce perceived contrast of central targets (Cannon and Fullenkamp, 1991; Snowden and Hammett, 1998; Xing and Heeger, 2000; Yu et al., 2001; Petrov and McKee, 2006). The fMRI response in human V1 is also reduced during surround suppression (Williams et al., 2003; Zenger-Landolt and Heeger, 2003; Pihlaja et al., 2008; Nurminen et al., 2009; McDonald et al., 2010; Chen, 2014).

The majority of existing fMRI studies of surround suppression have employed blocked experimental designs (Williams et al., 2003; Zenger-Landolt and Heeger, 2003; Pihlaja et al., 2008; Nurminen et al., 2009; McDonald et al., 2010), with multiple stimuli from a single condition presented repeatedly within a block. Schumacher and Olman (2010) instead used an event-related design to measure the fMRI response during ODSS, with individual trials presented every 3-6 sec. They found that the V1 fMRI response to small Gabor patches with parallel flankers did not increase with target contrast, and thus did not match the response predicted from psychophysics. This pattern was not observed with orthogonal flankers or when the target stimuli were large annular gratings, for which fMRI responses reliably increased with higher contrast. The most likely explanation for these results is that the V1 fMRI response reflected both the local stimulus features and

higher order pattern processing. However, the manner in which such pattern responses may depend on the structure and behavioral demands of the task performed during fMRI has yet to be determined.

The current study consists of a series of five experiments examining the role of stimulus geometry, attention, hemodynamics, and experimental design (blocked vs. event-related) during ODSS. We measured the blood oxygen level dependent (BOLD) response in early visual cortex to localized targets using high spatial resolution fMRI at 7 Tesla while manipulating both target contrast and the orientation of flanking context. While V1 fMRI responses with orthogonal surrounding stimuli increased as expected with higher target contrast, parallel condition responses showed little or no meaningful contrast sensitivity across experiments.

Methods

2.1 Participants

A total of 12 people (4 female and 8 male, mean age 31 years) participated across 5 experiments. Nine subjects participated in four of the experiments (referred to below as the *Attended Disks*, *SOA Gabors*, *Block Gabors*, and *Distracted Gabors* experiments). Seven of those subjects also took part in a fifth experiment, along with three additional participants (10 subjects total in the *Distracted Disks* experiment). All subjects had normal or corrected-to-normal vision. Five subjects were experienced psychophysical observers, and four of the subjects were the authors. The experimental protocol was approved by the University of Minnesota Institutional Review Board. Subjects gave their

written informed consent prior to participation, and those who were not authors were compensated $20 per hour.

2.2 Visual Stimuli

During fMRI, stimuli were projected on a screen mounted inside the bore of the magnet using a Sony VPL-PX10 or (following an equipment failure) NEC NP4100 projector and were viewed from a distance of 72 cm through a mirror mounted on the head-coil. Mean luminance was 158 cd/m^2 for the original and 79 cd/m^2 for the replacement projector. Display luminance was linearized using custom MATLAB (The Mathworks, Natick, MA) code. Stimuli were generated using PsychToolbox (Brainard, 1997; Pelli, 1997) and MATLAB on a Macintosh running OSX. Subjects made behavioral responses during the scan using a 4-button fiber optic response pad (Current Designs, Philadelphia, PA).

For the psychophysics experiment performed outside the scanner, stimuli from the *Disks* experiments (section 2.2.1) were viewed at a distance of 72 cm on a 21" NEC 2190UXi LCD monitor. A Bits++ digital video processor (Cambridge Research Systems, Kent, UK) provided 14-bit luminance resolution. Mean luminance was 95 cd/m^2. Display luminance was linearized using custom MATLAB code.

2.2.1 Disks

In the first two experiments (*Attended Disks* and *Distracted Disks*), stimuli consisted of a circular target surrounded on a subset of trials by an annulus (Figure 2-1A).

Targets and surrounds were sinusoidally modulated luminance gratings with a spatial frequency of 3 cycles per degree. This stimulus geometry has been used extensively to investigate the neural and perceptual mechanisms of ODSS (Cavanaugh et al., 2002; Shushruth et al., 2013). Target gratings with a radius of 0.75° were presented in all four quadrants of the screen at 3° eccentricity from a central fixation mark (white square, 8 pixels in diameter). Target stimulus orientation was either 45° or 315° from vertical, and thus gratings were aligned in a radial direction with respect to fixation. Surround annuli were 0.75° wide with an outer radius of 1.875°. Stimulus mask edges were blurred with a Gaussian envelope ($\sigma = 0.094°$). This blurring reduced the 0.375° gap between target and surround to a small low-contrast gap (approximately 0.1° wide, average contrast was half that of the target). Surrounding annuli were always presented at 50% contrast with an orientation that was either parallel (0°) or orthogonal (90°) to the surrounded target. When parallel, targets and surrounds had the same spatial phase.

2.2.2 Gabors

Stimuli presented in the other three experiments (*SOA Gabors*, *Distracted Gabors*, and *Block Gabors*; Figure 2-1B) matched those used by Schumacher and Olman (2010). Target stimuli were Gabor elements ($\sigma = 0.25°$; full width at half-maximum of 0.6°) with a spatial frequency of 3 cycles per degree. Four target Gabors were presented at 3° eccentricity, one in each visual quadrant, oriented 45° or 315° from vertical, aligned radially toward fixation. On a subset of trials, two flanking Gabors (same spatial frequency and bandwidth) were presented with each target Gabor, positioned 1° (center-

to-center) from the corresponding target along a tangential axis relative to fixation. Flanking Gabors were always presented at 50% contrast, with an orientation that was either parallel (0°) or orthogonal (90°) to the flanked target.

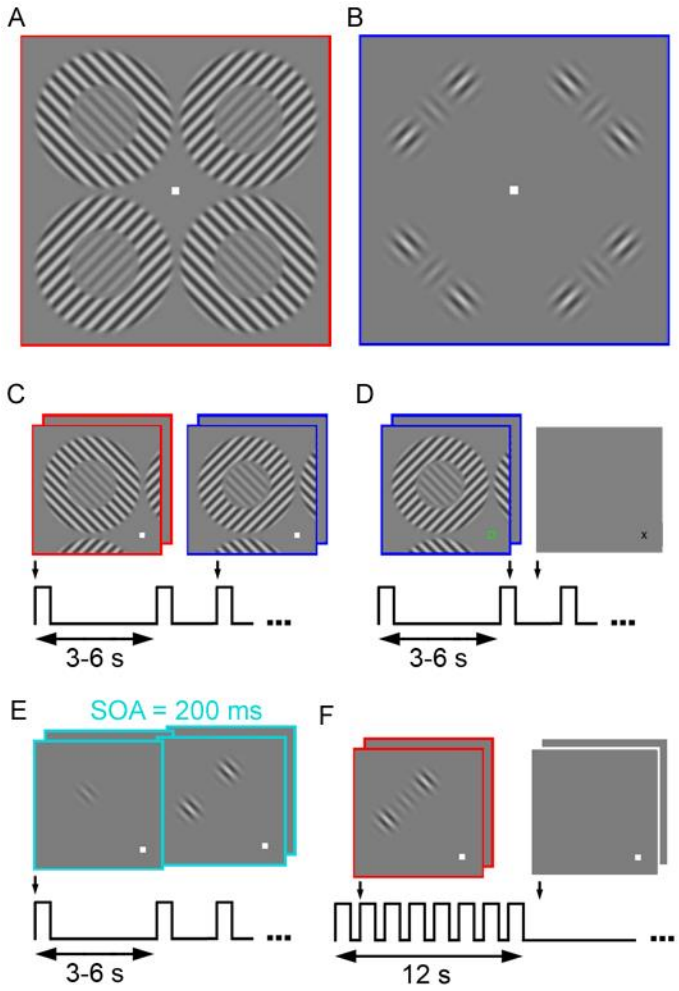

Figure 2-1. Stimuli and presentation paradigms.
A) Disks stimuli. B) Gabors stimuli. C) *Attended Disks* event-related paradigm, showing stimuli in one quadrant. D) *Distracted Disks* paradigm. Note the fixation task timing is independent from that of the peripheral gratings. E) *SOA Gabors* paradigm, illustrating the 200 msec stimulus onset asynchrony. F) *Block Gabors* blocked paradigm.

2.3 Paradigm

Each experiment measured fMRI responses during eight stimulus conditions. All experiments included a Target Alone condition in which the Michelson contrast of the targets was 16%, and a Surround Alone condition with surrounds presented at 50% contrast. The remaining six conditions were combinations of 3 pedestal contrast levels (8%, 16%, and 32%) and 2 surround configurations (parallel and orthogonal in the *Disks*, *Block Gabors*, and *Distracted Gabors* experiments; parallel with stimulus-onset asynchrony of 0 msec and 200 msec in the *SOA Gabors* experiment). Subjects were instructed to keep their eyes on the fixation mark at the center of the screen throughout each experiment. Each scanning session for each experiment contained 8 fMRI scans: two functional localizers used for region of interest (ROI) definition, and 6 task scans during which the 8 experimental conditions were presented.

2.3.1 Attended Disks experiment

During the *Attended Disks* experiment task scans, the stimuli were presented in an event-related paradigm (Figure 2-1C), with trial-onset intervals of 3 sec, 4.5 sec or 6 sec (uniformly and randomly distributed). Trials were composed of two 150 msec stimulus presentations (intervals), each followed by a mean luminance background presented for 750 msec. The 8 conditions were interleaved randomly, with 10 trials for each condition per scan. Task scan duration was 6.25 min. For one subject in this experiment, task scans were longer (299 TRs, 7.2 min), with stimuli from each of the eight conditions presented

12 times, plus an additional 12 presentations of the Surround Alone condition. In this case, only 4 task scans were completed.

During the task scans subjects performed a 2-interval forced-choice (2IFC) task, responding to a contrast increment in one of the four target stimuli during one of the two intervals. The target quadrant and the interval for which the contrast was augmented were both randomly assigned. In the Target Alone condition the pedestal contrast was 16%; in conditions with targets and surrounds, pedestal contrasts were 8%, 16% and 32%; in the Surround Alone condition, pedestal contrast was 0%. For all conditions, the contrast increment varied between trials (starting value 7.3%, range 1.6 - 40%), and was controlled by independent 3-down 1-up staircases, converging on 79% accuracy (Garcia-Perez, 1998) in order to control task difficulty. Feedback was given after each trial for 200 msec, with the fixation mark turning green for correct responses or red for incorrect responses.

Because of the small number of trials and the difficulty of performing a rapid discrimination task in the scanner, contrast discrimination thresholds measured during scanning were significantly higher than thresholds measured in behavioral sessions outside the scanner (section 2.4). However, thresholds during scanning were higher in the presence of parallel versus orthogonal surrounds or no surround (data not shown), consistent with behavioral data acquired outside the scanner. This reflects the expected ODSS during contrast perception within the scanning sessions (Yu et al., 2003). As there were 4 target positions in each of two stimulus presentation intervals, the true average contrast for each target was larger than the pedestal contrast by approximately $1/8^{th}$ of the

threshold contrast increment. Across all the conditions and subjects analyzed, there was an average increase in target contrast of 1.4% in the *Attended Disks* experiment.

2.3.2 Distracted Disks experiment

In the *Distracted Disks* experiment, circular gratings with annular surrounds were presented in an event-related paradigm as in the *Attended Disks* experiment. In this experiment, subjects were instructed to ignore the disks and instead to focus their attention on a demanding reaction time task presented at fixation (Figure 2-1D). Subjects monitored the central fixation point for the brief presentation of a black "X". The objective of the task was for subjects to press a button before the X disappeared, in order to earn or retain points (starting value 10). Prior to presentation of the fixation target, a colored fixation mark cue appeared for a variable duration (1.5 to 3.5 sec). Cues indicated both that a target was about to appear and that correct performance during the subsequent fixation trial would allow the subject either to win a single point (green square cue) or to prevent the loss of a point (red square cue). Failing to respond quickly enough on a win-trial had no effect on the point total, while failing on a loss-trial cost subjects one point. After each fixation trial, feedback was given for 500 msec (X turned green when earning a point, red when losing, and blue for no change), and then the current point total was displayed for 500 msec. Fixation task trials appeared every 5-7 sec and their timing was independent of the Gabor stimulus presentation. Fixation task difficulty was adjusted between scans by shortening the duration for which the X was presented, in order to ensure the attentional demands of the task were sufficiently high. The duration of the X at

the beginning of a scanning session was 400 msec. If accuracy during the previous scan was greater than 66%, the X stimulus duration was reduced by 50 msec, and if accuracy was less than 33%, the duration was increased by 50 msec. Accuracy was moderate across subjects (mean 64%, S.E.M. 7.1%), suggesting they were engaged in the task but not performing at ceiling.

2.3.3 SOA Gabors experiment

In the *SOA Gabors* experiment task scans, target Gabors were presented with parallel flanking Gabors that appeared with a stimulus-onset asynchrony (SOA) of either 0 msec or 200 msec (Figure 2-1E). Because target duration was 150 msec, targets and parallel flanking Gabors did not appear on the screen at the same time when SOA was 200 msec. The SOA of 200 msec was chosen because it is sufficiently long to minimize orientation-dependent masking by the surround (Ishikawa et al., 2006) but too short to interfere with sluggish hemodynamic effects, such as blood-stealing by regions outside the target ROI (Shmuel et al., 2002; Zenger-Landolt and Heeger, 2003; Smith et al., 2004a). Data from one task scan in one subject from *SOA Gabors* experiment were excluded because the scan was terminated early. The event-related paradigm matched that of *Attended Disks* experiment and subjects performed the same 2IFC contrast discrimination task (i.e., attention directed to the target Gabor stimuli). During scanning, larger contrast increments were observed in this task for the 0 msec SOA compared to the 200 msec SOA condition, as expected (Ishikawa et al., 2006). On average, target contrast increased by 2.2% due to the 2IFC task.

2.3.4 Distracted Gabors experiment

In the *Distracted Gabors* experiment, parallel and orthogonal flanking Gabor stimuli were presented in an event-related paradigm matching the *Disks* and *SOA Gabors* experiments. Subjects performed the demanding fixation task from the *Distracted Disks* experiment (Figure 2-1D), in order to divert attention away from the Gabor stimuli. Accuracy on this task was moderately high (mean 69%, S.E.M. 4.0%), and comparable with the *Distracted Disks* experiment.

2.3.5 Block Gabors experiment

During task scans in the *Block Gabors* experiment, parallel and orthogonal flanking Gabor stimuli were presented in a mixed block design (Figure 2-1F). In this experiment, one trial consisted of two 150 msec stimulus presentations with a 500 msec inter-stimulus interval, and a trial-onset interval of 1.5 sec. Subjects performed the same 2IFC contrast discrimination task as in the event-related design, except the feedback duration in this experiment was 100 msec. Stimuli from each condition were grouped in 12 sec blocks (8 trials per block) presented in a pseudo-random order, with two blocks of each condition presented in every scan. Each scan began with a 12 sec block during which a mean luminance blank screen was presented, and a blank block followed each stimulus block. Blank blocks consisted of 8 trials during which no flanking Gabors were present, and the pedestal contrast was 0% while subjects performed a 2IFC contrast detection task. The structure of the blank blocks equated attentional and task demands

between blank and stimulus blocks, with the former serving as the response baseline in this experiment. Each task scan in this experiment lasted 6.6 min. Contrast increments in the 2IFC task during scanning tended to be higher for parallel versus orthogonal surrounds, as in the *Attended Disks* experiment. This task led to an average increase in target contrast of 2.8%.

2.3.6 Functional Localizers

Disks experiments included functional localizer scans in which Target Alone stimuli alternated with Surround Alone stimuli in a block design (12 sec per block, 8 Target Alone and 9 Surround Alone blocks; total scan duration 3.2 min). This differential localizer approach was used in order to minimize signal displacement from the surrounding region into the target ROI (Olman et al., 2007). Disk and annulus stimuli matched the geometry used during task scans, and were presented at 80% contrast. The task during these localizer scans was the same as in Target Alone and Surround Alone conditions in the *Disks* experiments, but with a 125 msec stimulus duration, 250 msec inter-stimulus interval, and 1.5 sec trial-onset interval. The functional localizer for the Gabors experiments was a single-condition localizer, with 12 sec blocks of 80% contrast target Gabors (same timing and task structure as above) alternating against 12-sec blank blocks of 0% pedestal contrast target Gabors.

2.4 Analysis of behavioral data

In order to estimate the magnitude of the orientation-dependent surround suppression for the *Disks* experiment, we conducted a thorough investigation of contrast discrimination performance outside the scanner in a subset of 3 subjects using the concentric disk stimuli from the *Disks* experiments. Contrast discrimination thresholds for Target Alone, Parallel and Orthogonal conditions were measured at pedestal contrasts of 0% (detection), 1%, 2%, 4%, 8%, 16% and 32%. When present, surrounds were displayed at 50% contrast. Thresholds were determined using the Psi adaptive staircase procedure (Prins and Kingdom, 2009), averaging the threshold values obtained in 3 separate runs, each composed of 40 trials. Thresholds were estimated by fitting a Logistic function using a Maximum Likelihood criterion and calculating the fit value at 73% accuracy; threshold estimates smaller than 0.01% or larger than 14% contrast were excluded (5 data points total). Independent threshold versus contrast (TvC) curves were fit to data from the Target Alone, Parallel and Orthogonal conditions across 7 pedestal contrasts using Equation 2-1 (Boynton et al., 1999; Yu et al., 2003) via MATLAB's *lsqcurvefit*.

$$R = A * C^p / (C^{p-q} + \sigma^{p-q})$$

Equation 2-1

R is the predicted threshold and *C* is the pedestal contrast.

Table 2-1 shows the best fit parameters for the average TvC data from 3 subjects. Contrast-response functions (CRFs) were quantified as the integral of the fit TvC curve.

Table 2-1. Threshold versus contrasts parameters.
Parameters were fit using Equation 2-1 for the average psychophysical results from 3 subjects presented in Figure 2-2.

Condition	*A*	*p*	*q*	σ
Target Alone	175	1.61	0.49	1.00
Parallel surround	175	3.30	0.41	0.35
Orthogonal surround	175	2.49	0.44	0.40

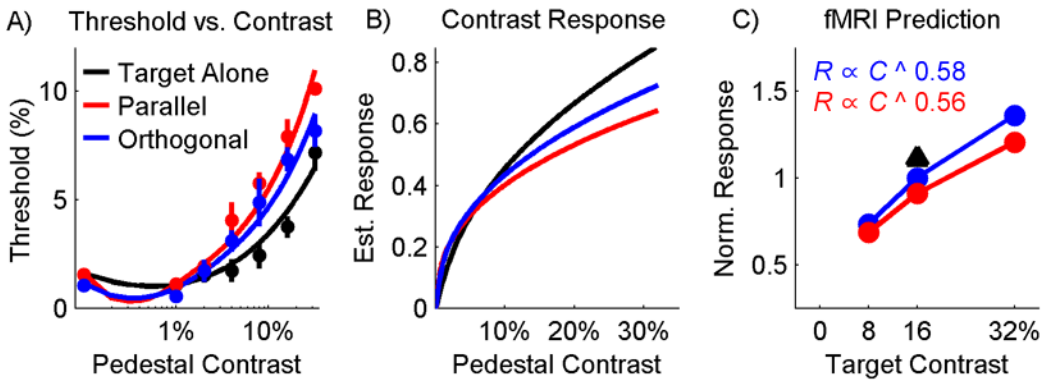

Figure 2-2. Psychophysics results and predictions.
A) Contrast discrimination thresholds for *Disks* stimuli obtained outside the scanner, and best-fitting TvC curves. Error bars show S.E.M. across subjects. B) Estimated *Disks* contrast-response functions. C) Predicted pattern of fMRI responses for *Disks*, normalized to a mean of 1. A power law was used to describe contrast sensitivity; the exponents shown were obtained by fitting Disks contrast-response functions from (B) using Equation 2-2. Orthogonal proportionality shown above Parallel.

Psychophysical contrast discrimination thresholds (averaged across 3 subjects) for the *Disks* stimuli are shown in Figure 2-2A. For each subject, thresholds were significantly larger for parallel than for orthogonal surrounds across all pedestal contrasts (paired 1-tailed *t*-test, $t_{(17\text{-}19)}$ values > 2.1, *p*-values < 0.036, FDR corrected). CRFs predicted from TvC curves (Figure 2-2B) showed the expected nonlinear response across the range of target contrasts used in our fMRI experiments (8-32%). Figure 2-2C shows the pattern of fMRI responses for the *Disks* stimuli predicted from the CRFs. Response amplitudes were normalized to a mean value of 1.

2.5 Imaging data acquisition

FMRI data were collected at the University of Minnesota's Center for Magnetic Resonance Research on a Siemens 7 Tesla scanner equipped with head-only gradients having a maximum strength of 80 mT/m and a slew rate of 333 T/m/s. A custom-made radio frequency head coil (4-channel transmit, 9-channel receive; Adriany et al., 2012) was used for gradient echo (GE) echo-planar imaging (EPI). Images were acquired with a coronal field of view (FOV) in 18 slices (1.2 mm thick) positioned near the occipital pole (Figure 2-3A). Image resolution was 1.2 mm isotropic; data were acquired with an in-plane parallel imaging acceleration factor (R) of 2. Due to acoustic noise limitations following gradient maintenance, the following EPI acquisition parameters varied slightly between scanning sessions: coverage, matrix size, echo time (TE), echo spacing, and partial Fourier (listed in Table 2-2). The repetition time (TR) was 1.5 sec. Task scans had 250 TRs in the *Disks*, *SOA Gabors*, and *Distracted Gabors* experiments, and 264 TRs in the *Block Gabors* experiment, while functional localizer scans had 136 TRs in all experiments. Total scanning time in each experiment was approximately 1 hr.

Table 2-2. EPI scan parameters.
For each experiment, the number of subjects (# Subj.) scanned with the listed parameters is noted in the second column. FOV = field of view (imaging coverage in mm). TE = echo time (in msec).

Experiment	# Subj.	FOV (mm)	Matrix Size	TE (msec)	Echo Spacing (msec)	Partial Fourier
Attended Disks	5	154 x 125	128 x 104	20	0.57	8/8
Attended Disks	4	154 x 135	128 x 112	20	0.70	7/8
Distracted Disks	10	154 x 135	128 x 112	20	0.70	7/8

SOA Gabors	5	154 x 154	128 x 128	18	0.52	7/8
SOA Gabors	4	154 x 135	128 x 112	20	0.70	7/8
Block Gabors	5	154 x 154	128 x 128	18	0.52	7/8
Block Gabors	4	154 x 135	128 x 112	20	0.70	7/8
Distracted Gabors	5	154 x 125	128 x 104	20	0.57	8/8
Distracted Gabors	4	154 x 135	128 x 112	20	0.70	7/8

2.6 Imaging data processing

During a separate scanning session, a 1 mm isotropic T_1-weighted anatomical scan was acquired, and a retinotopic mapping experiment (Engel et al., 1997; Larsson and Heeger, 2006) was performed for each subject. Anatomical images were used to generate gray and white matter surface definition files (SurfRelax; Larsson, 2001). Occipital patches from inflated white matter surfaces were computationally flattened and used to visualize functional data when defining regions of interest (ROIs). The retinotopy data were used to functionally identify early visual areas (V1-3).

Imaging data were first converted from DICOM to NIFTI pair format (dinifti; http://cbi.nyu.edu/software/dinifti.php). Head motion was corrected using an iterative least-squares method (AFNI's 3dvolreg; Cox and Jesmanowicz, 1999). Geometric distortion compensation was conducted using a field map scan acquired during the EPI scanning session (FSL's FUGUE; Smith et al., 2004b). Further data processing and analysis, including registration of the functional data to the T_1 anatomy (Nestares and Heeger, 2000) was completed using custom software in MATLAB.

2.7 Functional localization of target ROIs

Within retinotopically defined early visual areas (V1-3), ROIs were identified from the average of two functional localizer scans. Prior to averaging, the first 8 frames of each localizer scan were discarded to ensure activation did not reflect artifacts related to scan onset. Functional localizer scans were detrended by removing the first two Fourier components, and the two scans were then averaged. The Fourier transform of the average localizer time series was used to calculate the amplitude and phase of the response at the stimulus frequency (8 cycles / scan; Engel et al., 1997). Coherence (unsigned correlation) with stimulus presentation was computed as the 8 cycle / scan response amplitude divided by the square root of the time series power. Activation was classified as significant above a threshold coherence level of 0.3 (uncorrected *p*-value < 6×10^{-4}, assuming temporally uncorrelated noise). Phase values within a window of π to 1.6π (6-10 sec peak response lag) were used to identify positive fMRI responses in phase with the target stimulus presentation. Within each visual area, ROIs consisting of up to four sub-ROIs were identified based on the position of significantly activated in-phase voxels on the flattened cortical surface. These consisted of dorsal and ventral sub-ROIs in the left and right hemispheres, corresponding to the four target stimulus positions (one in each quadrant). ROIs were then translated to the space of the in-plane functional images for manual refinement, which ensured that sub-ROIs consisted of a cluster of contiguous, significantly activated voxels (Figure 2-3B, C, & D).

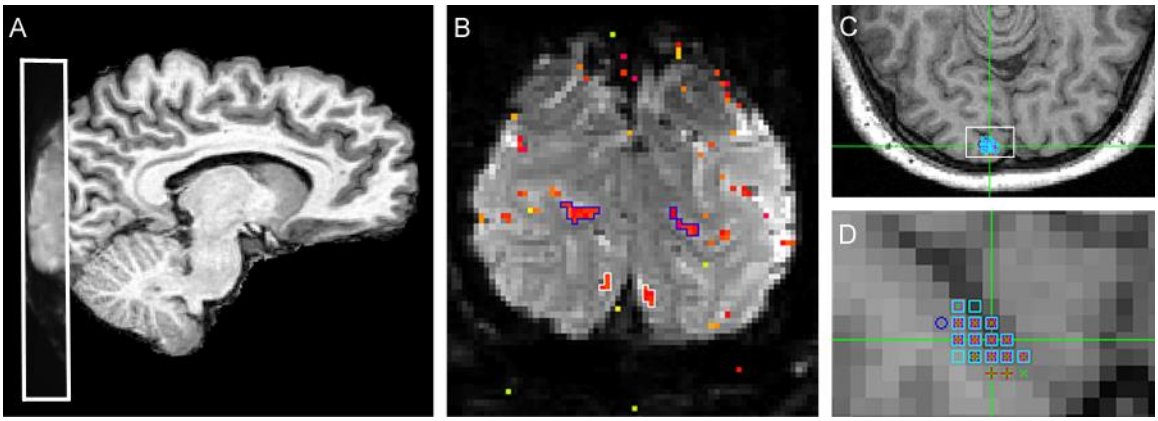

Figure 2-3. Functional images and ROI localization.
A) Sagittal view of structural MRI with EPI data overlaid to show imaging coverage and alignment. Functional slice prescription is outlined. B) In-plane view of functional data. V1 target ROIs (ventral, bilateral) and V2 target ROIs (dorsal, bilateral) are outlined. C) Axial view of structural MRI showing resampled positions for left ventral sub-ROI in V1 for five experiments. Voxels from the *Attended Disks* experiment are diamonds, *Distracted Disks* are squares, *SOA Gabors* are pluses, *Distracted Gabors* are circles, and *Block Gabors* are x-marks. Crosshairs indicate the center of mass across experiments, white box indicates the region magnified in (D).

The average number of sub-ROIs within V1-3 and the number of voxels they contained is listed for all experiments in Table 2-3. It was not always possible to identify four separate in-plane sub-ROIs in all early visual areas for every subject. In particular, V3 sub-ROIs were identified least reliably. In some subjects, ventral sub-ROIs beyond V1 could not be identified due to insufficient imaging coverage in the anterior-posterior direction. As expected, the differential functional localizer for the *Disks* experiments produced smaller ROIs than the single-condition localizer used in the *Gabors* experiments. The restriction of ROI size by the differential localizer was most striking in V2 and V3. This may be due to larger receptive field sizes in extrastriate areas (Smith et al., 2001), which would be expected to limit the number of voxels that selectively respond to target but not surround stimuli (Olman et al., 2007). Because of the small and

inconsistent nature of the extrastriate ROIs in the *Disks* experiments, V2 and V3 ROIs in these two experiments were not analyzed further.

From published estimates of average cortical magnification factors in human visual cortex (Engel et al., 1997), we would expect a circular stimulus with a radius of 0.75 deg. presented at 3 deg. eccentricity (as in the *Disks* experiments) to elicit an fMRI response across an approximately cylindrical region of V1, extending through the depth of the gray matter with a radius of 4 mm. Note, however, that V1 surface area and cortical magnification can vary by as much as a factor of two between subjects (Duncan and Boynton, 2003). Assuming an average V1 cortical thickness of 2.5 mm, a 4-mm radius would predict an average volume of activation of 126 mm^3, or about 73 voxels at 1.2 mm isotropic resolution. The average sub-ROI size in the *Disks* experiments was smaller than this, thus our differential localizer method was successful in identifying voxels that selectively responded to the target over the surround. Similarly, the target Gabor stimulus in the *Gabors* experiments (approximately 1 deg. wide) would be expected to activate a 2.7 mm radius cylindrical portion of V1, for an activation volume of 57 mm^3, or about 33 voxels. V1 sub-ROIs were smaller than this for the *Gabors* experiments on average, from which we conclude that our sub-ROI definition was conservative in these experiments as well, including only the most strongly modulated voxels representing the centers of the target Gabors.

Table 2-3. Sub-ROI statistics.
Sub-ROIs is the average number identified across subjects. # Voxels indicates the average number of voxels within each sub-ROI. Numbers in parentheses are standard deviation.

	V1	V2	V3

Experiment	# Sub-ROIs	# Voxels	# Sub-ROIs	# Voxels	# Sub-ROIs	# Voxels
Attended Disks	3.7 (0.5)	17 (10)	2.4 (1.1)	8 (11)	1.3 (0.7)	4 (3)
Distracted Disks	3.5 (0.7)	16 (13)	2.2 (1.3)	5 (13)	0.6 (0.8)	2 (1)
SOA Gabors	3.7 (0.7)	25 (15)	3.6 (0.7)	32 (17)	2.6 (0.9)	41 (40)
Block Gabors	3.8 (0.4)	22 (7)	3.3 (0.7)	32 (16)	2.4 (0.5)	41 (38)
Distracted Gabors	3.8 (0.4)	31 (18)	3.6 (0.5)	43 (26)	2.8 (0.7)	48 (66)

2.8 Analysis of fMRI data

FMRI data from task scans were analyzed using a general linear model (GLM). AFNI's 3dDeconvolve (Cox, 1996) was used to estimate the fMRI response (percent signal change from baseline) for each of the 8 stimulus conditions in all voxels. Nuisance regressors were modeled using the 6 motion parameters (roll, pitch, yaw, displacement in x, y and z) estimated during motion correction, as well as Legendre polynomials up to third order to remove temporal trends up to 1/150 sec. The AFNI program 1d_tool.py was used to censor TRs in which there was excessive motion (defined as a Euclidean norm of the temporal derivative for the 6 motion parameters above 0.3). For one subject who participated in all 5 experiments, a large proportion of TRs were censored (26% on average); this subject was excluded from all experiments due to unreliable data (see below). For all other subjects, 2.4% of TRs were censored on average (SD = 1.5%), or about 6 TRs per scan.

Response amplitude estimates were averaged across all voxels in each ROI. For the event-related experiments, hemodynamic response functions (HRFs) were assessed separately for each subject and condition at 12 time points (18 sec) following stimulus onset, and the fMRI response amplitude was quantified as the average response between 3 and 4.5 seconds post-stimulus (the peak response). For the *Block Gabors* experiment,

individual HRFs were not estimated; instead a canonical HRF (SPM; Friston et al., 1994) was used to model the BOLD response, and amplitude was estimated as the beta weight for each condition regressor. A few subjects in each experiment showed particularly weak fMRI responses and noisy HRFs. In order to exclude these unreliable data sets, we calculated the average *t*-statistic for the estimated response amplitude across all 8 stimulus conditions in each subject. Within every experiment, we retained the 7 subjects with the highest average *t*-statistics, and excluded the rest (3 subjects in *Distracted Disks*, 2 subjects in every other experiment).

The following analyses were conducted using MATLAB. Raw fMRI response amplitudes were compared across conditions and experiments using a 2-way analysis of variance (ANOVA), with subjects treated as a random effect. Responses in each ROI for each subject were then normalized in the following manner: First, responses were divided by the subject's mean response across all 8 stimulus conditions, to remove contributions of experiment design and individual variability in overall response amplitude. Then the Surround Alone response was subtracted to account for non-specific fMRI responses to the surround within the target ROI. Note that Surround Alone responses were not subtracted from Target Alone condition. Normalized fMRI response amplitudes were compared in a 3-way ANOVA across surround conditions, target contrasts, and experiments. Contrast (8, 16, and 32%) was treated as a continuous variable. False discovery rate (FDR) correction was used to adjust *p*-values from post-hoc tests for multiple comparisons.

In order to characterize fMRI contrast sensitivity, we fit responses with the exponential function shown in Equation 2-2 using MATLAB's *lsqcurvefit*.

$$R = a * C^b$$

Equation 2-2

This power law models the neural response *R* as the product of a scalar variable *a* and the target contrast *C* raised to the exponent *b*. Responses in each surround condition (e.g., Parallel and Orthogonal) were fit separately. The Surround Alone condition was included as a baseline during fitting.

This contrast response analysis depends on a few assumptions that should be explicitly considered. First, we assume that non-specific responses to the surround within the target ROI are additive, and thus can be accounted for by subtracting the Surround Alone response during normalization. In essence, this assumes equal non-specific surround responses regardless of the target contrast. While we cannot rule out some dependence of surround responses on the target, this assumption is consistent with previous studies (Zenger-Landolt and Heeger, 2003; Pihlaja et al., 2008). We additionally assume that non-specific responses are equal for all surround conditions (e.g., Parallel & Orthogonal), and that the Surround Alone condition provides a good estimate for these non-specific responses.

We used this same power law analysis to examine contrast response functions (CRFs) predicted from psychophysics (Figure 2-2C). Responses were fit by contrast response exponents of 0.56 and 0.58 for Parallel and Orthogonal *Disks*, respectively. We also fit this power law to psychophysical CRFs obtained for the *Gabors* in our previous

study (Schumacher and Olman, 2010). Across Parallel and Orthogonal conditions in both studies, the average exponent value was 0.58. These results agree with psychophysical (Legge and Foley, 1980; Legge, 1981) and electrophysiological (Albrecht and Hamilton, 1982) work reporting CRF exponents in the range of 0.6.

Results

In five experiments we examined how factors such as target contrast, spatial context, stimulus geometry, attention, hemodynamics, and experimental design influenced the local fMRI response in visual cortex. Functional MRI data from 7 subjects were examined in each experiment. We used 1.2 mm GE EPI at 7 Tesla, in order to achieve high spatial resolution imaging across early visual cortex with high BOLD contrast-to-noise ratio (Olman and Yacoub, 2011). Responses in small regions of interest (ROIs) corresponding to the cortical representation of target stimuli were measured while varying both the central target contrast and surrounding stimulus configuration.

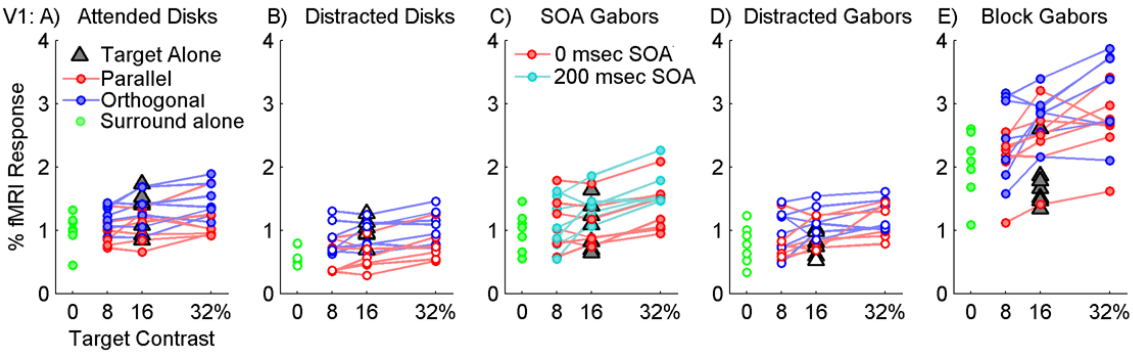

Figure 2-4. Raw V1 fMRI responses.
Amplitudes are shown for 8 conditions across 5 experiments in 7 subjects. Lines connect responses from the same subject at different target contrast levels. Filled symbols indicate attention directed to the target stimuli, open symbols indicate attention directed toward a fixation task.

Table 2-4. Statistical analyses of raw fMRI responses.
A 2-way ANOVA compared response amplitudes from 5 experiments across 8 conditions in 7 subjects. Bold indicates a significant effect at $\alpha = 0.05$.

Raw fMRI responses

Analysis	Test	Statistic	Significance
A. Experiment	**ANOVA – Main Effect**	$\boldsymbol{F_{(4,30)} = 31.2}$	$\boldsymbol{p < 0.001}$
i. Disks: Distracted < Attended	**Post-hoc *t*-test**	$\boldsymbol{t_{(110)} = 6.91}$	$\boldsymbol{p^{\dagger} < 0.001}$
ii. Gabors: Distracted < Attended	**Post-hoc paired *t*-test**	$\boldsymbol{t_{(34)} = 3.76}$	$\boldsymbol{p^{\dagger} < 0.001}$
iii. Gabors: SOA < Block	**Post-hoc paired *t*-test**	$\boldsymbol{t_{(34)} = 9.11}$	$\boldsymbol{p < 0.001}$
B. Condition	**ANOVA – Main Effect**	$\boldsymbol{F_{(7,30)} = 50.6}$	$\boldsymbol{p < 0.001}$
C. Experiment x Condition	**ANOVA – Interaction**	$\boldsymbol{F_{(28,210)} = 6.12}$	$\boldsymbol{p < 0.001}$
i. Disks: Surround Alone < Target Alone	**Post-hoc paired 1-tailed *t*-tests**	$\boldsymbol{t_{(6)} \geq 3.07}$	$\boldsymbol{p^{\dagger} < 0.011}$
ii. Gabors: Surround Alone ≈ Target Alone	Post-hoc paired 1-tailed *t*-tests	$t_{(6)} \leq 0.56$	$p^{\dagger} > 0.8$

† FDR corrected for multiple comparisons.

3.1 Raw fMRI responses in V1

We first used a 2-way ANOVA to compare raw V1 fMRI responses from 5 experiments across 8 stimulus conditions in 7 subjects (Figure 2-4; Table 2-4). We expected responses would vary across experiments in the following manner: First, larger responses were anticipated with attention directed toward versus away from the target stimuli (Buracas and Boynton, 2007; Li et al., 2008b; Murray, 2008). As expected, *Attended Disks* responses (across all 8 conditions) were larger than *Distracted Disks* (Table 2-4.A.i). Likewise, attended responses for *SOA Gabors* were larger than those in the *Distracted Gabors* (Table 2-4.A.ii; across 5 conditions, 200 msec SOA and

Orthogonal were not compared due to stimulus differences). Second, we anticipated larger responses for blocked versus event-related designs (Huettel et al., 2009). *Block Gabors* responses were indeed larger than *SOA Gabors* (Table 2-4.A.iii; across 5 conditions as above). Thus, attending the target stimuli and the use of a blocked design each increased the overall fMRI response amplitude in V1.

When comparing responses in different stimulus conditions, we examined how well V1 target ROIs were isolated from the surrounding region by testing whether Target Alone responses were larger than Surround Alone. We predicted that the differential localization method (section 2.7) used in the *Disks* experiments would produce better-isolated ROIs than those obtained from the single-condition localizers in the *Gabors* experiments (Olman et al., 2007). Consistent with this prediction, responses were larger for Target Alone versus Surround Alone in the *Disks* (Table 2-4.C.i) but not the *Gabors* (Table 2-4.C.ii).

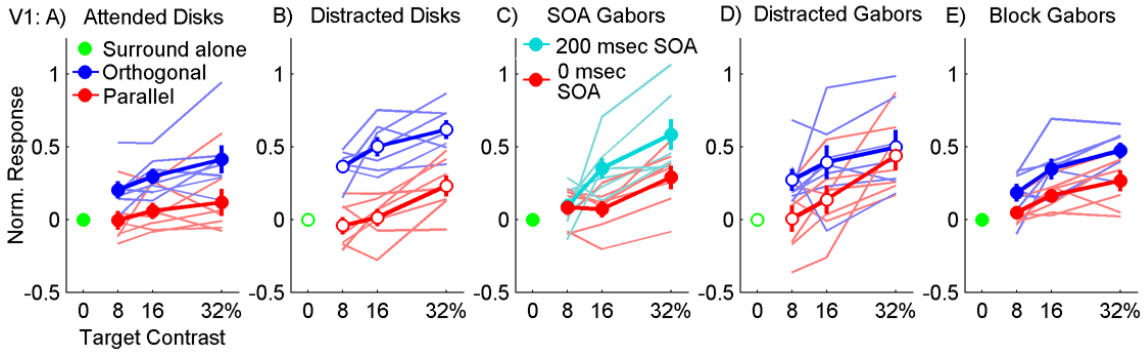

Figure 2-5. Normalized fMRI responses in V1.
For each subject, response amplitudes were normalized to a mean of 1 across all 8 conditions, and then responses to the Surround Alone condition were subtracted. Thin lines show data from individual subjects, circles and thick lines show group means, error bars show S.E.M. Filled symbols indicate attention directed to the target stimuli, open symbols indicate attention directed toward a fixation task.

Table 2-5. Statistical analysis of normalized V1 fMRI response amplitudes.

A 3-way ANOVA compared responses across 5 experiments, 2 surround configurations, and 3 target contrasts in 7 subjects. Bold indicates a significant effect at $\alpha = 0.05$, italics indicate a trend at $\alpha = 0.10$.

Normalized fMRI responses

Analysis	Test	Statistic	Significance
A. Experiment	ANOVA – Main Effect	$F_{(4,30)} = 0.92$	$p = 0.4$
B. Surround Configuration	**ANOVA – Main Effect**	$\mathbf{F_{(1,30)} = 25.4}$	$\mathbf{p < 0.001}$
i. Block Gabors, Distracted Gabors, Attended Disks, Distracted Disks: Parallel < Orthogonal	**Post-hoc paired *t*-tests**	$\mathbf{t_{(20)} \geq 3.83}$	$\mathbf{p^{\dagger} < 0.001}$
ii. SOA Gabors: 0 msec < 200 msec SOA	**Post-hoc paired *t*-test**	$\mathbf{t_{(20)} = 3.66}$	$\mathbf{p = 0.0015}$
C. Contrast	**ANOVA – Main Effect**	$\mathbf{F_{(1,30)} = 102}$	$\mathbf{p < 0.001}$
D. Experiment x Surround	**ANOVA – Interaction**	$\mathbf{F_{(4,30)} = 3.43}$	$\mathbf{p = 0.020}$
i. Disks (Orthogonal – Parallel): Attended < Distracted	**Post-hoc *t*-test**	$\mathbf{t_{(12)} = 3.17}$	$\mathbf{p^{\dagger} = 0.016}$
ii. Distracted (Orthogonal – Parallel): Gabors < Disks	**Post-hoc *t*-test**	$\mathbf{t_{(12)} = 4.92}$	$\mathbf{p^{\dagger} < 0.001}$
E. Experiment x Contrast	ANOVA – Interaction	$F_{(4,60)} = 1.57$	$p = 0.2$
F. Surround x Contrast	ANOVA – Interaction	$F_{(2,60)} = 0.35$	$p = 0.5$
G. Experiment x Surround x Contrast	*ANOVA – Interaction*	$F_{(4,30)} = 2.43$	$p = 0.069$

† FDR corrected for multiple comparisons.

3.2 Normalized V1 fMRI responses

We normalized fMRI responses in each individual subject by dividing out the subject's mean response across all 8 stimulus conditions and then subtracting the Surround Alone response. This allowed us to compare how responses in different experiments depended on target contrast and surround configuration, while controlling for differences in overall response magnitude and non-specific fMRI responses to the surround. We used a 3-way ANOVA to compare normalized fMRI responses in V1 across 5 experiments, 2 surround conditions and 3 target contrasts in 7 subjects (Figure 2-5; Table 2-5). For all experiments and surround conditions, larger normalized V1

responses were generally observed with greater contrast (Table 2-5.C.i) as anticipated (Boynton et al., 1996; Boynton et al., 1999; Zenger-Landolt and Heeger, 2003; Olman et al., 2004; Schumacher et al., 2011a). However, this effect was modulated by experimental conditions and surround configuration, as shown below.

Lower responses were observed for Parallel versus Orthogonal surrounding stimuli (i.e., orientation-dependent surround suppression, ODSS; Table 2-5.B.i), as expected (Williams et al., 2003; Pihlaja et al., 2008; McDonald et al., 2010). In the *SOA Gabors* experiment, we expected larger responses with 200 msec versus 0 msec SOA (Zenger-Landolt and Heeger, 2003), consistent with neural suppression of the target response by simultaneous but not delayed parallel flanking Gabors. Responses were indeed larger with delayed surround onset (200 msec SOA) versus simultaneous surrounds (0 msec SOA; Table 2-5.B.ii). Additionally, surround suppression was stronger in some experiments than in others (Table 2-5.D). Of the 10 possible post-hoc comparisons, we examined 2 for which a difference in ODSS may be attributed to a change in a single experimental condition between experiments. We calculated the difference in normalized responses between Orthogonal and Parallel conditions for all target contrasts, and compared this difference across separate experiments. Previous work suggests that attending to target stimuli decreases ODSS (Zenger et al., 2000). Consistent with this prediction, we observed stronger ODSS in the *Distracted Disks* experiment versus *Attended Disks* (Figure 2-5A & B; Table 2-5.D.i). We also expected stronger ODSS for *Disks* versus *Gabors*, because the surrounding stimuli were larger (Pihlaja et al., 2008; Nurminen et al., 2009). Stronger ODSS was observed for the *Distracted Disks*

versus *Distracted Gabors* (Figure 2-5B & E; Table 2-5.D.ii). However it is not clear whether this effect holds for attended stimuli; we could not address this question, as attended Orthogonal Gabor responses were not measured in an event-related design. Finally, we observed a trend-level 3-way interaction between experiment, surround condition, and target contrast for the normalized V1 responses (Table 2-5.G). Examining this interaction more closely allowed us to determine how the V1fMRI response to target contrast was affected by surrounding stimuli across different experiments.

3.3 V1 fMRI contrast sensitivity

We characterized the contrast response in V1 across different experiments and surround conditions using an exponential function (Equation 2-2; reprinted in Figure 2-6B). Contrast-response functions are well described by this kind of power law model; exponents (*b*) near 0.6 are predicted from human psychophysics (Legge and Foley, 1980; Legge, 1981) and animal electrophysiology (Albrecht and Hamilton, 1982). This agrees with our psychophysical contrast response functions for the *Disks* (Figure 2-2B & C) and *Gabors* (Schumacher and Olman, 2010; their Figure 2), which followed a power law with an average exponent of 0.58 (section 2.8).

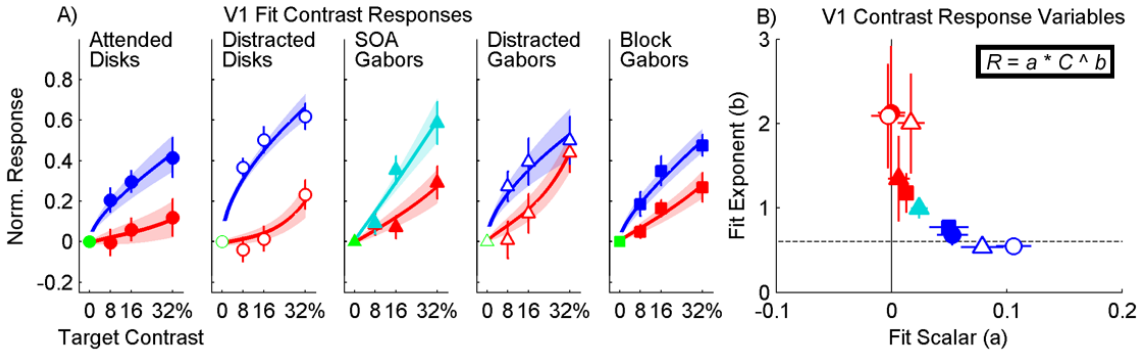

Figure 2-6. V1 fMRI contrast sensitivity.
A) Normalized V1 fMRI responses were fit with an exponential function using Equation 2-2 reprinted in (B). Lines show the mean and shaded regions show the S.E.M. of the curves across subjects. Symbols show mean normalized responses, error bars show S.E.M. (identical to the data in Figure 2-5). Filled symbols indicate attention directed to the target stimuli, open symbols indicate attention directed toward a fixation task. B) Variables obtained from fitting. Symbols match (A).

Using the exponential function in Equation 2-2, we fit normalized fMRI responses at 0 (Surround Alone baseline), 8, 16, and 32% target contrast from 2 surround configurations across 5 experiments in 7 subjects (Figure 2-6A). The variable *b* characterized the exponential shape of the fMRI response across target contrast *C*, while the variable *a* served as a multiplicative scalar. Orthogonal exponents (*b*) clustered around the expected value of 0.6 across all experiments, indicating good agreement between Orthogonal fMRI responses and the predicted power law (Figure 2-6B). Parallel exponents (*b*) were large in all experiments (often > 1, indicating an accelerating response), and highly variable across subjects. Further, Parallel scalar values (*a*) were clustered around zero, indicating that responses between 8-32% contrast do not increase much beyond the Surround Alone baseline. Together, these results indicate that Parallel fMRI responses in our paradigms cannot be modeled by the predicted power law. Finally, 200 msec SOA condition showed exponent values around 1, which indicates a linear

contrast response rather than the expected saturation. This last result suggests that the 200 msec delay only partially eliminated interactions between the target and the surrounds.

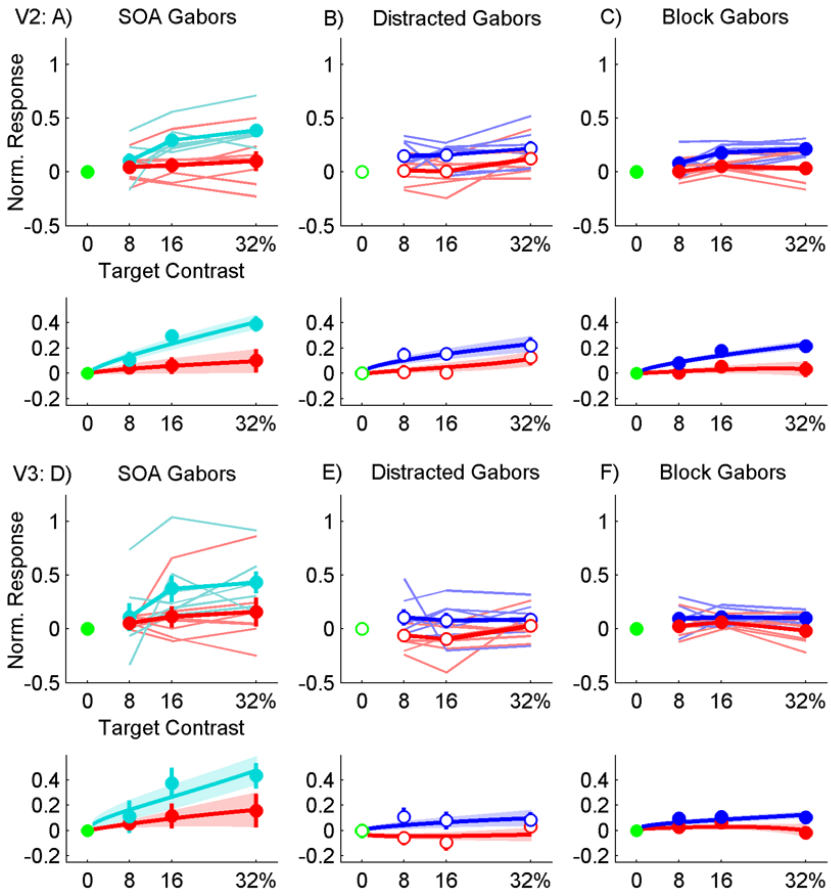

Figure 2-7. V2 and V3 results.
Normalized fMRI responses in V2 (A-C) and V3 (D-F). Circles show mean responses, error bars show S.E.M. Filled symbols indicate attention directed to the target stimuli, open symbols indicate distraction. Thin lines in first row panels show individual subject data. In second row panels, lines show mean fit contrast response across subjects, shaded regions show S.E.M.

Table 2-6. Statistical results from analyses of V2 and V3 fMRI responses.
Raw responses were compared in 2-way ANOVAs across 3 experiments and 8 stimulus conditions in 7 subjects. Normalized responses were examined in 3-way ANOVAs across 3 experiments, 2 surround configurations, and 3 target contrasts in 7 subjects. Bold indicates a significant effect at $\alpha = 0.05$, italics indicate a trend at $\alpha = 0.10$.

V2 and V3 Results

Analysis	Test	Statistic	Significance
A. Raw fMRI responses in V2 and V3			
i. Experiment	**ANOVA – Main Effects**	$\mathbf{F_{(2,18)} \geq 21.4}$	$\mathbf{p < 0.001}$
a. V2 Gabors: Distracted < Attended	*Post-hoc paired t-test*	$t_{(34)} \leq 1.91$	$p^{\dagger} = 0.065$
b. V3 Gabors: Distracted ≈ Attended	Post-hoc paired *t*-test	$t_{(34)} = 0.51$	$p^{\dagger} = 0.6$
c. V2 & V3 Gabors: SOA < Block	**Post-hoc paired *t*-tests**	$\mathbf{t_{(34)} \geq 10.7}$	$\mathbf{p^{\dagger} < 0.001}$
ii. Condition	**ANOVA – Main Effects**	$\mathbf{F_{(7,18)} \geq 32.2}$	$\mathbf{p < 0.001}$
iii. Experiment x Condition	**ANOVA – Interactions**	$\mathbf{F_{(14,126)} \geq 8.33}$	$\mathbf{p < 0.001}$
a. V2 & V3 Gabors: Surround Alone ≈ Target alone	Post-hoc paired 1-tailed *t*-tests	$t_{(6)} \leq -0.30$	$p^{\dagger} > 0.9$
B. V2 normalized fMRI responses			
i. Experiment	ANOVA – Main Effect	$F_{(2,6)} = 0.01$	$p = 0.9$
ii. Surround Configuration	**ANOVA – Main Effect**	$\mathbf{F_{(1,6)} = 4.57}$	$\mathbf{p = 0.046}$
a. Block Gabors, Distracted Gabors: Parallel < Orthogonal	**Post-hoc *t*-tests**	$\mathbf{t_{(20)} \geq 4.15}$	$\mathbf{p^{\dagger} < 0.001}$
b. SOA Gabors: 0 msec < 200 msec	**Post-hoc *t*-test**	$\mathbf{t_{(20)} = 4.64}$	$\mathbf{p < 0.001}$
iii. Contrast	**ANOVA – Main Effect**	$\mathbf{F_{(1,6)} = 37.7}$	$\mathbf{p < 0.001}$
iv. Experiment x Surround	ANOVA – Interaction	$F_{(2,12)} = 1.13$	$p = 0.3$
v. Experiment x Contrast	ANOVA – Interaction	$F_{(2,12)} = 2.23$	$p = 0.136$
vi. Surround x Contrast	**ANOVA – Interaction**	$\mathbf{F_{(1,12)} = 4.41}$	$\mathbf{p = 0.050}$
vii. Experiment x Surround x Contrast	*ANOVA – Interaction*	$F_{(2,12)} = 3.25$	$p = 0.063$
C. V3 normalized fMRI responses			
i. Experiment	ANOVA – Main Effect	$F_{(2,6)} = 1.28$	$p = 0.3$
ii. Surround Configuration	ANOVA – Main Effect	$F_{(1,6)} = 1.81$	$p = 0.196$
iii. Contrast	**ANOVA – Main Effect**	$\mathbf{F_{(1,6)} = 11.4}$	$\mathbf{p = 0.0034}$
iv. Experiment x Surround	ANOVA – Interaction	$F_{(2,12)} = 0.67$	$p = 0.5$
v. Experiment x Contrast	**ANOVA – Interaction**	$\mathbf{F_{(2,12)} = 9.32}$	$\mathbf{p = 0.0017}$
vi. Surround x Contrast	ANOVA – Interaction	$F_{(1,12)} = 0.29$	$p = 0.5$
vii. Experiment x Surround x Contrast	ANOVA – Interaction	$F_{(2,12)} = 1.23$	$p = 0.3$

† FDR corrected for multiple comparisons.

3.4 Responses in V2 and V3

FMRI responses were also measured in extrastriate areas V2 and V3, however ROIs in these areas could not be reliably identified in the *Disks* experiments because the differential localizer produced such small regions of activation (see section 2.7 and Table 2-3). Therefore, V2 and V3 fMRI responses were examined only in the *Gabors* experiments. When comparing raw fMRI response amplitudes across experiments (data not shown), we expected larger responses with attention and for the blocked experimental design, as in V1. While blocked responses were larger than event-related in V2 and V3 (Table 2-6.A.i.a), attended responses were only marginally larger than distracted in V2 (Table 2-6.A.i.b & c). We also expected poor isolation of target ROIs from surrounding regions due to the single-condition localizer and large receptive fields in V2 and V3. This was demonstrated by the fact that Target Alone responses were not larger than Surround Alone in V2 and V3 (Table 2-6.A.iii.a).

After normalizing V2 and V3 fMRI responses (Figure 2-7), we observed the expected ODSS (McDonald et al., 2010) and SOA-dependent suppression (Zenger-Landolt and Heeger, 2003) in V2 (Table 2-6.B.ii), but not V3 (Table 2-6.C.ii). Contrast sensitivity was weak but significant in V2 and V3 (Table 2-6.B.iii & C.iii), consistent with previous findings (Zenger-Landolt and Heeger, 2003). Interactions between surround and contrast in V2, and experiment and contrast in V3 were driven by strong contrast sensitivity in the 200 msec SOA condition of *SOA Gabors*. Indeed, fit contrast responses in V2 and V3 showed very weak contrast sensitivity in general (Figure 2-7,

second row panels), with strong contrast sensitivity observed only in the 200 msec SOA condition.

Discussion

We conducted five fMRI experiments to quantify surround suppression with different stimulus geometry, focal attention, surround onset timing, and experimental design (blocked versus event-related). We observed a larger difference in normalized V1 fMRI response between Orthogonal and Parallel conditions when attention was directed away from versus toward the *Disks* target stimuli. This indicated that attention decreased the magnitude of ODSS in the V1 fMRI response relative to the mean response amplitude. A reduction in ODSS by attention may serve to increase the salience of central targets, and aid segmentation of targets from similar background stimuli (Zenger et al., 2000). To our knowledge, this is the first direct observation of attention reducing ODSS in human V1. However, Zenger and colleagues (2000) observed stronger perceptual ODSS during contrast discrimination when subjects performed a concurrent distracting fixation task, versus when target Gabors were fully attended. Weaker V1 fMRI responses to peripheral checkerboards have also been observed during more difficult fixation tasks, consistent with stronger surround suppression in the periphery with greater attentional demands at fixation (Schwartz et al., 2005). Finally, pharmacological enhancement of acetylcholine (a neuromodulator implicated in visual attention; Sarter et al., 2005; Newman et al., 2012) has been found to reduce perceptual ODSS (Kosovicheva et al.,

2012). All of these reports are consistent with our finding of weaker ODSS in V1 with attention directed toward target gratings versus a distracting fixation task.

Our results also replicated a number of well-known effects from past fMRI studies of early visual processing. As expected, directing attention toward the target stimuli led to an overall increase in response amplitudes across conditions within a retinotopic region of V1, compared to when subjects performed a demanding fixation task (Kastner et al., 1998; Tootell et al., 1998; Brefczynski and DeYoe, 1999; Ress et al., 2000; Müller and Kleinschmidt, 2004; Schwartz et al., 2005; Buracas and Boynton, 2007; Silver et al., 2007; Li et al., 2008b; Murray, 2008; Bouvier and Engel, 2011; Bressler et al., 2013; Runeson et al., 2013). Using a blocked experimental design also increased response amplitudes across early visual areas V1-3 compared with an event-related paradigm (Huettel et al., 2009). Consistent with ODSS, fMRI responses in V1 were suppressed when targets were presented with more-similar surrounding stimuli (e.g., parallel versus orthogonal; Williams et al., 2003; Zenger-Landolt and Heeger, 2003; Pihlaja et al., 2008; McDonald et al., 2010; Chen, 2014). Finally, while V1 responses were sensitive to target contrast (at least in the presence of orthogonal surrounding stimuli, see below; Boynton et al., 1996; Boynton et al., 1999; Zenger-Landolt and Heeger, 2003; Olman et al., 2004; Schumacher et al., 2011a), V2 and V3 responses varied little with contrast, except when the surround onset was delayed by 200 msec, in agreement with previous findings (Zenger-Landolt and Heeger, 2003). These results reflect the strong influence of attention, target contrast, and surrounding context on the V1 fMRI response.

A major focus of the current study was to characterize how the V1 fMRI response to target contrast depends on surrounding stimulus context. Psychophysical measurements demonstrated ODSS of perceived contrast, and predicted larger responses for higher target contrasts (see Figure 2 and psychophysical data from Schumacher and Olman, 2010; their Figure 2). Both our psychophysical results and previous studies of visual contrast-response functions (Legge and Foley, 1980; Legge, 1981; Albrecht and Hamilton, 1982) indicated that the fMRI response in V1 should follow a power law with an exponent around 0.6, regardless of surrounding context. However unlike our predictions, we found that the V1 fMRI response did not consistently reflect changes in target contrast (8-32%) under all conditions. While contrast responses for orthogonal stimuli followed the expected power law (exponents around 0.6), parallel condition responses were not well modeled by such an exponential function, and showed little or no increase above the baseline measured in the Surround Alone condition. This indicates that suppression by parallel surrounds overwhelmed sensitivity to target contrast in the V1 fMRI response by reducing responses to a level near (or in some cases, below) this baseline non-specific response to the surround. In other words, when there was no orientation difference between target and surround, the V1 fMRI response in the target region was dominated by signals representing the surround. In the absence of the segmentation cue provided by orthogonal surrounds, responses in the target region appeared to strongly represent grouping of the target and parallel surrounds, rather than the actual contrast of the target.

The *SOA Gabors* experiment was designed to test the hypothesis that neural suppression (and not hemodynamic effects) produced surround suppression in the V1 fMRI response. Presenting the flanking Gabors 200 msecs after the targets increased the fMRI response relative to simultaneous targets and flankers. This is consistent with the 200 msec SOA disrupting neural ODSS (Ishikawa et al., 2006), but would not be expected if suppression depended on sluggish hemodynamics (Zenger-Landolt and Heeger, 2003). However, contrast response exponents for the 200 msec SOA condition were larger than expected, which suggests that the 200 msec delay was not long enough to completely eliminate neural interactions between targets and parallel surrounds.

Comparing between the *Disks* and *Gabors* experiments allowed us to examine how stimulus geometry affected the V1 fMRI response to target contrast during ODSS. A previous study reported monotonically increasing V1 fMRI responses for large stimuli with parallel surrounds (i.e., a circular annulus 3.3° wide, spanning ~11 mm on the cortical surface; Zenger-Landolt and Heeger, 2003), and our group was able to replicate this finding (Schumacher and Olman, 2010; their Figure 7). However, in the same study fMRI responses actually *decreased* with target contrast for small Gabor stimuli (~1° wide, ~5 mm on the cortical surface) with parallel (but not orthogonal) flankers (Schumacher and Olman, 2010; their Figure 4). In the current study, the *Disks* experiments employed concentric grating stimuli that were larger than the Gabor patches but smaller than the annular gratings used in previous studies. We did observe an effect of stimulus geometry on ODSS; the *Distracted Disks* experiment showed relatively stronger ODSS when compared with *Distracted Gabors*. However our results in all

experiments showed little or no increase in the V1 fMRI response above baseline for 8-32% contrast targets with parallel surrounds, regardless of geometry. Thus, our *Disks* target stimuli were not sufficiently large to produce reliable contrast responses as measured by fMRI in V1.

In summary, our results show that the magnitude of ODSS in the V1 fMRI response is reduced when subjects directs attention toward the target stimuli. We also found that while fMRI contrast response functions in V1 for targets with Orthogonal surrounds followed the expected power law, responses to targets with parallel surrounds did not. This highlights the challenge of measuring meaningful fMRI contrast responses using small stimuli that evoke strong surround suppression.

Chapter 3 :

Reduced Contextual Effects on Visual Contrast Perception in Schizophrenia and Bipolar Affective Disorder

Authors: Michael-Paul Schallmo, Scott R. Sponheim, and Cheryl A. Olman

To be submitted to *Schizophrenia Bulletin*

Summary

The perceived luminance contrast of a visual stimulus is often reduced by nearby stimuli. This surround suppression effect may help locate object edges by enhancing subtle differences between objects and backgrounds. Previous work has shown weaker surround suppression among people with schizophrenia. Studying this deficit may help identify impaired neural processing mechanisms in schizophrenia, as the neurobiology of the visual system is relatively well known. By examining surround suppression among subjects with schizophrenia or bipolar affective disorder, their unaffected biological relatives, and healthy controls we sought to determine whether diminished surround suppression was specific to schizophrenia, and if subjects with a genetic risk for either disorder would show similar deficits. Measuring perceived contrast in different surround conditions allowed us to additionally investigate how this suppression depends on the similarity of center and surrounding stimuli. We found weaker surround suppression among patients with schizophrenia, regardless of surround configuration. Subjects with bipolar affective disorder showed an intermediate deficit, with stronger suppression than

in schizophrenia but weaker than control subjects. Relatives of patients with either disorder showed normal performance. This is the first observation that reduced surround suppression is associated with both schizophrenia and bipolar affective disorder, but not with a genetic risk for these disorders. Further, our results indicate this impairment is not sensitive to the configuration of surrounding stimuli, implicating a deficit in broadly-tuned (rather than sharply orientation- or direction-selective) suppression mechanisms. This deficit is consistent with impaired suppression at an early stage of visual processing (e.g., LGN or V1).

Introduction

The human visual system exhibits context-specific processing, such that the neural response to an object depends on nearby objects or backgrounds. One well-studied example of this is known as surround suppression, wherein the response to an object is reduced in the presence of similar nearby stimuli (Cavanaugh et al., 2002). The perceived contrast (difference in brightness) of a target is also reduced by surrounds with similar features (orientation, direction of motion; Snowden and Hammett, 1998; Yu et al., 2001), an effect that is reminiscent of camouflage. Surround suppression is believed to play an important role in visually detecting edges and distinguishing objects from backgrounds.

Patients with schizophrenia (SZ) show a number of visual processing abnormalities including hallucinations, and it has been suggested that studying these impairments may provide insight into the neural underpinnings of this disorder, as visual neuroscience is relatively well-studied (Butler et al., 2008; Phillips and Silverstein, 2013;

Yoon et al., 2013; Notredame et al., 2014). A number of recent studies have shown weaker surround suppression among SZ patients compared with healthy controls (HC; Dakin et al., 2005; Tadin et al., 2006; Yoon et al., 2009; Tibber et al., 2013; Yang et al., 2013). However, it is not clear whether this deficit is specific to SZ, or if it is also observed in other psychiatric conditions, such as bipolar affective disorder (BP). Further, it is not known whether persons with a genetic risk for such disorders, such as first-degree biological relatives of schizophrenia (SZrel) or bipolar affective disorder patients (BPrel), show similar deficits in surround suppression. Finally, the extent to which diminished surround suppression in SZ depends on the similarity between targets and surrounding stimuli is not well established.

The current study examines suppression of visual contrast perception by surrounding stimuli among SZ and BP patients, SZrel, BPrel, and HC subjects, to determine whether deficits in surround suppression are present in each group. We varied the configuration of surrounding stimuli to examine how such deficits depend on the similarity between center and surround. While surround suppression was impaired for SZ and to a lesser extent BP patients, unaffected relatives showed no deficit, indicating that such abnormalities are not closely linked to genetic risk for these disorders, and thus may not serve as endophenotypes. Weaker surround suppression may instead reflect the extent to which psychiatric disease processes impair healthy functioning at an early level of visual processing.

Methods

Participants

Thirty-two outpatients with schizophrenia (SZ), 1 patient with schizoaffective disorder – depressed type (grouped with SZ for analysis), 23 patients with bipolar disorder (BP), 7 patients with schizoaffective disorder – bipolar type (grouped with BP), 28 unaffected first-degree biological relatives of schizophrenia patients (SZrel), 11 unaffected first-degree biological relatives of bipolar patients (BPrel), 10 unaffected first-degree biological relatives of patients with schizoaffective disorder – bipolar type (grouped with BPrel), and 45 healthy control subjects (HC) were recruited to participate in this study. Diagnoses were made by a doctorate-level clinical psychologist using the DSM-IV-TR (APA, 2000), Structured Clinical Interview for DSM Disorders (First, 1997), and Psychosis Module from the Diagnostic Interview for Genetic Studies (Nurnberger et al., 1994). Following consensus diagnosis, one SZrel and one BPrel were found to have diagnoses of SZ and BP, respectively. We retained these subjects in the relative groups, as re-running our analyses with them excluded yielded an equivalent pattern of results. Additionally, we re-ran our analyses excluding schizoaffective disorder – bipolar type patients, to explore whether grouping them with BP patients affected our pattern of results. Equivalent results were obtained once again, thus we opted to keep these subjects in the BP group.

The following exclusion criteria were used during subject recruitment: English as a second language, mental retardation, history of central nervous system disorder, head trauma with significant loss of consciousness, electroconvulsive therapy, current alcohol

abuse or drug dependence. All subjects had normal or corrected-to-normal visual acuity. HC subjects had no history of schizophrenia, bipolar disorder, or other psychotic disorder diagnoses for themselves and their first-degree biological relatives. Subjects provided written informed consent prior to participation and were compensated $15 per hour. The experimental protocol was approved by the Institutional Review Boards of the University of Minnesota and the Minneapolis VA Medical Center.

Subjects reported their parents' level of education using a 7-point rating scale (Schallmo et al., 2013). IQ was estimated using the Wechsler Adult Intelligence Scale (WAIS-III; Jeyakumar et al., 2004). The following behavioral measures were used to assess psychiatric symptom levels: Brief Psychiatric Rating Scale (BPRS; Overall and Donald, 1962), Scale for the Assessment of Negative Symptoms (SANS; Andreasen, 1982), Scale of the Assessment of Positive Symptoms (SAPS; Andreasen, 1984), and Schizotypal Personality Questionnaire (SPQ; Raine, 1991). Medication levels were converted to chlorpromazine (CPZ), mood stabilizer, and anti-depressant equivalent doses (Andreasen et al., 2010).

Stimuli

Sine wave grating stimuli were generated using MATLAB (The MathWorks, Natick, MA) and Psychtoolbox (Brainard, 1997; Pelli, 1997) on a MacMini running OSX, and were displayed on a 19 inch Dell monitor that subtended 35.1 x 26.7 degrees of visual angle at a viewing distance of 61cm. Display luminance was linearized using custom software. Mean luminance was 84 cd/m^2. Center stimuli comprised two circular

sine wave grating patches 1° in diameter, with a spatial frequency of 2 cycles per degree, presented at 2° eccentricity to the left and right of a central fixation mark (blue square 8 pixels across) along the horizontal meridian. Gratings drifted at a rate of 3.75 cycles per second. The orientation of the central grating and direction of stimulus motion was randomly assigned on each trial from an even distribution of 4 possible orientations between 0 and 135°, each with 2 relative directions of motion (0 or 180°).

Different stimulus conditions were defined by the presence and configuration of an annular sine wave grating stimulus surrounding one of the circular gratings (Figure 3-1). We refer to the center presented with the surround as the target, and the center presented alone as the reference. We included different surround conditions in order to examine how similarity between target and surrounds (e.g., orientation, direction of motion) would affect perception of target contrast. In the Parallel condition, surrounding gratings were parallel (0°) in orientation relative to the target stimuli, and had the same spatial phase. The inner diameter of the surround was 1°, so target and surround were abutting. The Gap condition was identical to the Parallel condition, except that a 0.1° mean luminance gap separated the target and surround. The addition of a gap was intended to mitigate the contribution of brightness induction on the perceived target contrast (Yu et al., 2001), effectively reducing the strength of surround suppression. In the Orthogonal condition, abutting target and surround stimuli were presented with an orthogonal or perpendicular (90°) relative orientation. The Opposite condition was identical to the Parallel condition, except that the stimuli in the target and surround drifted in opposite directions. Note that in Figure 3-1, this condition is illustrated with

target and surround having opposite spatial phase to convey that the opposite drift direction disrupts the relative phase relationship between the two. Both the Orthogonal and Opposite configurations were expected to reduce the magnitude of the surround suppression effect; previous experiments have demonstrated weaker surround suppression for centers and surrounds with different orientations or directions of motion (Yu et al., 2001; Cavanaugh et al., 2002; Paffen et al., 2005). Finally, there was a None condition in which no surround stimulus was presented. When present, the outer diameter of the surround was 3°. Surrounds were displayed at 70% Michelson contrast, and target contrast was 50%. The position of the target and surround versus reference stimuli (left or right) was randomly assigned on each trial.

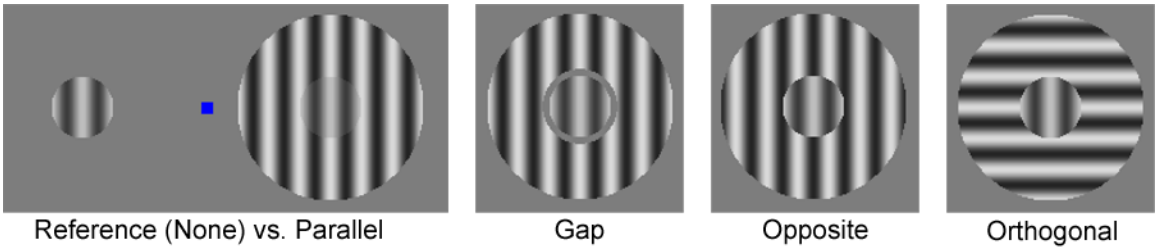

Figure 3-1. Surround suppression stimuli.
Left panel illustrates the stimulus layout, with Reference (left, no surround, identical to the None condition) and Parallel condition stimuli (right) offset horizontally from a central fixation square.

Paradigm

Subjects were asked to fix their eyes on the central square and use their peripheral vision to compare the contrast of the target and reference. In each trial, stimuli were presented for 300 msec, following which subjects indicated which center stimulus (left or right) was higher contrast by pressing the corresponding arrow key. Response time was

not limited. After a response was made there was a 400 msec interval prior to the next trial onset during which the fixation mark was displayed. Twenty-five trials were presented for each condition in a random intermixed order, which composed one run. Each subject completed at least 4 runs. Prior to the start of the experiment, subjects were shown a set of static example stimuli while the task was explained. Subjects were told that one center stimulus would sometimes be presented with a surround, but to focus on comparing the contrast of the two centers while ignoring the surround. Next, 15 practice trials were completed during which stimuli from the None condition were presented, followed by 15 practice trials with stimuli from the Gap condition. The total experiment duration including practice was approximately 10 minutes.

This task was designed to measure the perceived contrast of the target center. For the first 85 subjects, the contrast of the reference was adjusted across trials using a 1-up, 1-down staircase method to determine the point of subjective equality between perception of target and reference contrast. This method converges on the reference contrast perceived as higher 50% of the time (Garcia-Perez, 1998), which we refer to as the threshold contrast. For the remaining 72 subjects, reference contrast was adjusted across trials using the Psi adaptive staircase procedure to determine the threshold contrast (Prins and Kingdom, 2009). Thresholds were measured separately in each run for each surround condition, in order to determine how surrounding stimulus configuration affected target contrast perception. Reference contrast varied in a range between 14 and 74% contrast, with a starting point of either 40 or 60% (on alternating runs). Target contrast was always 50%.

Analysis

For data collected using the 1-up, 1-down staircase method described above, thresholds were defined as the average contrast from the last 6 trials in the staircase in each condition. For the Psi staircase data, the 50% threshold value and corresponding psychometric function slopes were calculated by fitting a Logistic function to the staircase responses using a Maximum Likelihood criterion (Prins and Kingdom, 2009). The guess rate and lapse rate were both set to 4%. Staircases with Psi thresholds values less than 0% or greater than 100% were excluded. Out of 1140 such staircases, 196 were excluded in this manner. We saw no significant difference in thresholds between the two staircase methods (ANOVA, $F_{(1,145)} = 0.13$, $p = 0.7$), therefore data from both were combined in all subsequent analyses.

We examined the distribution of thresholds using Kolmogorov–Smirnov and Levene's tests, which showed our data were normally distributed with equal variance across groups. Primary statistical analyses were performed using repeated measures analyses of variance (ANOVA), with subject treated as a random effect and nested within group. Post-hoc comparisons were conducted using Tukey's Honestly Significant Difference (HSD) test, or Pearson's correlation with Bonferroni correction for multiple comparisons. In order to quantify the relative effect of different surround configurations on contrast perception, contextual modulation indices were calculated by subtracting Parallel condition thresholds from thresholds in the Gap, Orthogonal, and Opposite conditions in each run for every subject.

Enhancement

A number of datasets acquired using either of the staircase methods showed thresholds around 70% (i.e., 20% enhancement relative to the 50% contrast target) for all or most of the conditions in which the surround was presented. This contradicts the well-established pattern of perceived contrast suppression for a central target presented with a higher-contrast surround (Snowden and Hammett, 1998; Yu et al., 2001). We believe that these subjects failed to follow the task instructions and erroneously compared the reference contrast to the surround contrast, which was 70% across conditions, thus producing thresholds that resembled enhancement of perceived target contrast. Therefore, data sets with three or more threshold values from surround-present conditions greater than or equal to 60% (averaged across runs), and zero thresholds less than or equal to 40%, were analyzed as a separate Enhancement group. Data from 10 SZ, 11 BP, 3 SZrel, 4 BPrel, and 7 HC subjects showed a pattern of enhancement; thus 23 SZ, 19 BP, 25 SZrel, 17 BPrel, and 38 HC subjects were retained in the final analyses.

The distribution of subjects exhibiting enhancement did not vary significantly across diagnosis groups ($X^2_{(4)} = 8.27$, $p = 0.082$). No differences in threshold were observed between conditions in which the surround was present (ANOVA, $F_{(3,30)} = 0.93$, $p = 0.4$). Further, thresholds did not differ across groups ($F_{(4,30)} = 1.78$, $p = 0.16$), and we did not observe a significant group by condition interaction ($F_{(16,120)} = 1.49$, $p = 0.11$), indicating that thresholds among Enhancement subjects did not depend on diagnosis group. Contextual modulation indices from the Enhancement group also did not vary

across condition ($F_{(2,30)} = 0.41$, $p = 0.6$), further demonstrating that surround modulation did not depend on stimulus configuration for these subjects. However, we did observe a significant difference in contextual modulation indices between groups ($F_{(4,30)} = 3.70$, $p = 0.013$); post-hoc tests indicated that the 3 SZrel subjects in the Enhancement group had higher contextual modulation indices than all other Enhancement subjects. Overall, data from the Enhancement group are not consistent with feature-selective surround modulation (Yu et al., 2001; Cavanaugh et al., 2002; Paffen et al., 2005), but instead appear to indicate that subjects were responding to surrounding stimulus contrast (70%), rather than perceived center target contrast (~50%). Failing to follow task instructions in this way would produce thresholds around +20% in all surround-present conditions regardless of stimulus configuration, as we observed. Data from the Enhancement group were excluded from further analyses.

Results

Statistical tests for differences between groups in demographics and self-report measures are reported in Table 3-1.

Table 3-1. Subject demographic information.
All data are presented as mean (standard deviation) unless otherwise noted. Data are presented for subjects retained in the final analyses. Bold indicates significant results at $\alpha = 0.05$, italics indicate a trend at $\alpha = 0.10$.

Index	**SZ (n = 23)**	**SZrel (n = 25)**	**BP (n = 19)**	**BPrel (n = 17)**	**HC (n = 38)**	**Statistics**
Age (years)	45 (9)	44 (11)	44 (11)	41 (14)	44 (12)	$F_{(4,117)} = 0.37$, $p = 0.8$
Gender (n)						**$X^2_{(4)} = 14.4$, $p = 0.0060$**
Male	18	8	15	11	23	

Female	5	17	4	6	15	
Education (years)	*13.7 (2.0)*	*14.6 (2.3)*	*14.2 (1.6)*	*14.4 (1.3)*	*15.2 (1.9)*	*$F_{(4,103)} = 2.11$, $p = 0.084$*
Parents' Education (7-point scale)	5.1 (1.2)	4.5 (1.1)	4.6 (1.2)	4.8 (0.7)	4.6 (1.3)	$F_{(4,113)} = 0.93$, $p = 0.4$
Estimated IQ	**93 (20)**	**104 (14)**	**105 (14)**	**113 (19)**	**106 (16)**	**$F_{(4,104)} = 3.50$, $p = 0.010$**
Overall Symptomatology (BPRS Total Score)	**47 (12)**	**31 (7)**	**39 (10)**	**34 (9)**	**28 (4)**	**$F_{(4,116)} = 22.1$, $p < 0.001$**
Schizotypal Characteristics (SPQ Total Score)	**35 (17)**	**7 (7)**	**24 (16)**	**16 (14)**	**7 (7)**	**$F_{(4,92)} = 19.7$, $p < 0.001$**
Negative Symptoms (SANS Total Score)	**36 (18)**		**19 (15)**			**$F_{(1,40)} = 11.5$, $p = 0.0016$**
Positive Symptoms (SAPS Total Score)	**26 (23)**		**10 (14)**			**$F_{(1,40)} = 6.68$, $p = 0.014$**
CPZ Equivalents	831 (831)		524 (554)			$F_{(1,23)} = 0.89$, $p = 0.3$
Mood-stabilizer Equivalents	636 (580)		700 (301)			$F_{(1,12)} = 0.07$, $p = 0.7$
Anti-depressant Equivalents	**259 (260)**		**63 (72)**			**$F_{(1,18)} = 5.80$, $p = 0.027$**

We sought to determine how surrounding stimulus configuration affected perception of target contrast among SZ and BP patients, their unaffected first-degree biological relatives, and healthy controls. To do so, we adjusted the contrast of a reference center stimulus using a staircase procedure to quantify the point of subjective equality between reference and target (threshold contrast). Five different center-surround stimulus conditions were used: Parallel, Gap, Opposite, Orthogonal, and None (Figure 3-1). Thresholds for each condition in each group following exclusion (see Methods) are presented in Figure 3-2, with SZ, BP, and HC groups shown together in Figure 3-2A, and

SZrel, BPrel, and HC groups in Figure 3-2B. Conditions are arranged in Figure 3-2 with greatest center-surround feature similarity (Parallel) on the left, to least (Orthogonal) on the right, followed by the None condition in which no surround was present.

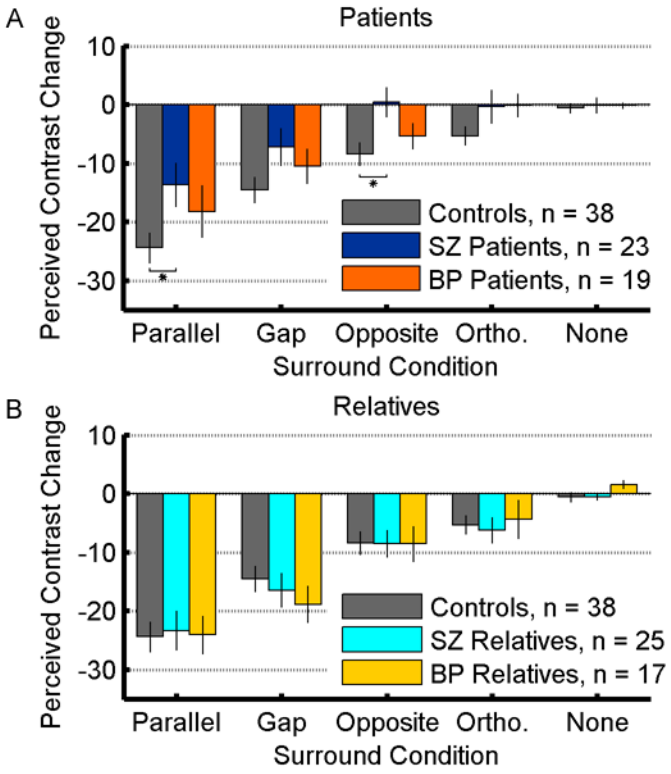

Figure 3-2. Surround suppression task thresholds.
A) Data from HC, SZ, and BP groups. Surround configurations are shown across the x-axis. Thresholds are plotted on the y-axis as the change in perceived contrast relative to the 50% contrast target; negative values indicate suppression. Error bars show the standard error of the mean (S.E.M.). Asterisks indicate significant differences in thresholds between groups (Tukey's HSD, $p < 0.05$). B) Data from HC, SZrel, and BPrel groups.

We first performed an omnibus analysis, using an ANOVA to compare threshold contrasts across all surround conditions and subject groups. A main effect of condition was observed ($F_{(4,117)} = 97.0$, $p < 0.001$), indicating that surround configuration significantly affected target contrast perception. Collapsing across groups, thresholds

differed significantly in post-hoc tests between each surround condition, with lower thresholds when center and surround were more similar (Parallel < Gap < Opposite < Orthogonal < None; Tukey's HSD, $p < 0.05$). This matches the expected form of configuration-dependent surround suppression (Yu et al., 2001; Cavanaugh et al., 2002; Paffen et al., 2005): greater feature similarity (e.g., orientation and direction of motion) evoked greater suppression of perceived center contrast. We also observed a main effect of subject group ($F_{(4,117)} = 2.70$ $p = 0.034$); post-hoc tests showed that SZ subjects had significantly higher thresholds than all other groups (averaged across all conditions), while BP subjects showed higher thresholds than HC, BPrel and SZrel groups, but smaller thresholds than SZ subjects ($p < 0.05$; Figure 3-2A). No differences in thresholds were observed between HC, SZrel and BPrel groups (Figure 3-2B). These results indicate that surround suppression is greatly diminished among SZ subjects (Dakin et al., 2005; Tadin et al., 2006; Yoon et al., 2009; Barch et al., 2012; Tibber et al., 2013), reduced among BP subjects (but less so than in SZ), and equally strong among relatives with a genetic risk for SZ or BP compared with HC subjects.

We next sought to determine whether suppression deficits among patients were more evident in certain conditions. Although the group by condition interaction was not significant ($F_{(16,465)} = 1.35$, $p = 0.16$), we conducted planned post-hoc tests for differences between groups within each surround condition. Post-hoc tests revealed significantly weaker suppression of perceived contrast in the Parallel and Opposite conditions among SZ versus HC, SZrel, and BPrel subjects (Tukey's HSD, $p < 0.05$). None of the other 44

comparisons between subject groups within each condition were significant using Tukey's HSD.

To further examine how surround similarity affected the strength of suppression, Contextual Modulation Indices were computed as the difference in perceived contrast between the Parallel and Gap, Orthogonal, or Opposite conditions. Indices differed across conditions as expected (2-way ANOVA, 3 conditions x 5 groups; $F_{(2,115)} = 76.6$, $p < 0.001$). However, we saw no significant effect of group ($F_{(4, 115)} = 0.25$, $p = 0.9$), and no interaction between group and condition ($F_{(8, 221)} = 1.25$, $p = 0.2$). These results indicate that different surround configurations evoked similar changes in contrast perception across all subject groups, relative to the Parallel condition.

We also examined relationships between task performance and subject demographic data to determine whether such factors might be related to the magnitude of surround suppression. Although gender composition differed across groups (Table 3-1), including gender as a between-subjects factor did not affect the results from our analysis of thresholds. Also, no significant correlations were observed between thresholds and any of the following factors: age, education, parents' education, symptomatology scores (BPRS, SANS, SAPS, and SPQ), or medication levels. We did observe significant negative correlations between estimated IQ and thresholds in the Parallel, Gap, and Opposite conditions ($r_{(105\text{-}107)} < 0.34$, $p = 0.016$, Bonferroni corrected). This indicates that across diagnosis groups, subjects with higher IQ showed stronger surround suppression in these conditions, consistent with recent findings in healthy subjects (Melnick et al., 2013). Because subjects in the Schizophrenia group had significantly lower IQ than those

in other groups (Table 3-1), we assessed the contribution of IQ to surround suppression by performing a secondary analysis. This analysis compared thresholds for subjects with IQ scores in the top 50^{th} percentile for each group. All such subjects had estimated IQ scores ≥ 99. This analysis again showed a significant difference in surround suppression between groups ($F_{(4,48)} = 3.29$, $p = 0.018$). Post-hoc tests revealed weaker surround suppression across conditions for SZ and BP subjects versus HC ($p < 0.05$), although the difference between BP and SZ was no longer significant. Across the high IQ sub-group, IQ scores were not significantly correlated with thresholds in any condition ($r_{(51)} < 0.2$, $p > 0.5$). Thus, IQ scores alone cannot account for our observation of diminished surround suppression among SZ and BP subjects.

Next, we chose to more closely examine whether the level of current psychotic symptoms among SZ and BP patients may be associated with deficits in surround suppression. Previous work has reported an association between reduced visual illusion strength and greater psychotic symptom levels (Keane et al., 2013). To examine this relationship in our paradigm, we calculated sub-indices of positive and manic symptoms based on responses from the BPRS, and similar scores for negative symptoms, thought disorders, or hallucinations and delusions based on responses to the SANS and SAPS (Wilson and Sponheim, 2014). These 5 sub-scores (BPRS positive, BPRS mania, SANS negative, SAPS thought disorder, and SAPS hallucinations / delusions) were examined for correlations with perceived contrast changes among SZ and BP patients. As we observed equivalent deficits among patients across surround conditions, sub-scores were correlated with the average change in perceived contrast from the Parallel, Gap,

Opposite, and Orthogonal conditions, in order to reduce multiple comparisons. Of the 10 correlations examined, none were significant ($r < 0.31$, $p > 0.153$, uncorrected). This suggests little or no relationship between current symptomatology and the magnitude of visual surround suppression among SZ and BP patients.

Finally, we sought to determine whether differences in thresholds between conditions and groups might be attributed to non-visual factors such as off-task performance (e.g., lapses of attention, lack of effort; see Barch et al., 2012; Tibber et al., 2013). To do so, we conducted two additional analyses, the first of which compared the standard deviations of the threshold measurements for each subject across the 4 runs. We supposed that if subjects in a particular group had a higher level of off-task performance, than this could lead to less stable threshold estimates, and greater threshold variability across runs. However, groups did not show significantly different threshold standard deviations ($F_{(4,117)} = 0.39$, $p = 0.8$). We also examined psychometric function slopes for subjects who completed the Psi staircase version of our task (see Methods). Greater slope values indicate a more reliable perceptual transition at the threshold contrast value; thus we expected that greater off-task performance would be associated with smaller (less reliable) slope values. We found no evidence for any difference in slopes across groups ($F_{(4,52)} = 0.66$, $p = 0.6$). While these results cannot disprove the notion that off-task performance contributed to the pattern of thresholds observed across subject groups, they do not lend support to it.

Discussion

The aim of this study was twofold: First, we investigated whether a putative deficit in surround suppression is specific to SZ or is also observed in BP and/or unaffected first degree biological relatives of patients. Second, we examined how such deficits might depend on similarity between center and surrounding stimuli. We observed overall weaker surround suppression of perceived contrast among patients with SZ, and to a lesser extent those with BP, compared with their unaffected relatives and HC subjects. The magnitude of this deficit did not depend strongly on the configuration of surrounding stimuli. Diminished surround suppression is fairly well established among SZ subjects, having been observed by a number of groups using different paradigms and stimuli (Dakin et al., 2005; Tadin et al., 2006; Yoon et al., 2009; Barch et al., 2012; Robol et al., 2013; Schallmo et al., 2013; Seymour et al., 2013; Tibber et al., 2013; Yang et al., 2013). Here we have demonstrated for the first time that BP patients also show weaker surround suppression, albeit to a lesser degree than those with SZ. Our results are also the first observation that the magnitude of perceptual surround suppression does not depend on genetic risk for SZ or BP, as SZrel and BPrel showed equivalent suppression to HC subjects.

Overall, we found little evidence to support a specific deficit in suppression for particular surround configurations; no group by condition interaction was observed for thresholds, and contextual modulation indices did not vary significantly across groups. The most parsimonious explanation for these results is that patients with SZ show a broad deficit in the strength of surround suppression that is not selective for surrounding

stimulus features. This proposal contrasts with previous findings showing weaker surround suppression in SZ for parallel but not orthogonal stimuli (Yoon et al., 2009; Seymour et al., 2013). However, those two studies employed larger (2.2 or 3.3° wide) lower spatial frequency (both 1.1 cycles per degree) annular gratings that were presented more peripherally (3.3 or 6.2° eccentricity) than our stimuli (1° diameter circular gratings, 2 cycles per degree, 2° eccentricity). One might therefore attribute this discrepancy to differential activation of neural pathways in early visual cortex tuned to particular stimulus features (e.g., a larger magnocellular contribution in processing the large, low frequency, peripheral stimuli in the previous studies). Our stimuli were not designed to be biased toward parvocellular (P) or magnocellular (M) processing, nor were those used by Yoon and colleagues (2009), as stated in their Discussion. Nevertheless, the stimulus differences may have been sufficient to yield divergent results.

It is not clear precisely how surround suppression depends on spatial frequency and eccentricity (Petrov and McKee, 2006), or M versus P pathways (Cudeiro and Sillito, 1996; Solomon et al., 2002). However, if surround suppression is stronger for M neurons (Solomon et al., 2002), or orientation selectivity of suppression is sharper at low spatial frequencies (Cudeiro and Sillito, 1996), then this may help explain the difference between our results and those of others noted above. It is worth noting that a specific deficit in M contrast sensitivity among SZ patients has been proposed (Butler et al., 2005), though this has been disputed (Skottun and Skoyles, 2007). Further study is warranted to clarify how M versus P pathways contribute to perceptual surround suppression in both the healthy visual system and in those with SZ.

Surround suppression is believed to be driven by multiple neural processes whose anatomical substrates include feed-forward, recurrent, lateral, and feedback connections within and between early visual cortical areas (e.g., primary visual cortex, V1; Angelucci and Bressloff, 2006; Shushruth et al., 2012). Previous work suggests that these separate processes include an early stage that is insensitive to the configuration of surrounding stimuli, and a later stage that is more sharply tuned (Paffen et al., 2005; Webb et al., 2005; Cai et al., 2008; Henry et al., 2013; Chen, 2014). This early stage produces a baseline level of suppression in the presence of a surrounding stimulus (regardless of configuration), and may operate at the level of the lateral geniculate nucleus of the thalamus, or at the input layers of primary visual cortex (Webb et al., 2005; Angelucci and Bressloff, 2006). The later stage is believed to evoke additional suppression with greater strength for surrounds that are more similar to the center stimulus, consistent with intracortical mechanisms that are more strongly selective for visual stimulus features. Thus, our observation of weaker suppression among SZ and BP patients across surround configurations appears consistent with a deficit in this putative early stage, suggesting an impairment in neural suppression at the level of the LGN or V1.

Abnormal inhibition by the neurotransmitter γ-ammino butyric acid (GABA) has been reported in SZ (Lewis et al., 2005; Gonzalez-Burgos and Lewis, 2008; Hashimoto et al., 2008; Yoon et al., 2010; Rokem et al., 2011; Kelemen et al., 2013). One study measured lower GABA concentrations in visual cortex among SZ versus HC subjects using magnetic resonance spectroscopy, and found lower GABA correlated with weaker surround suppression (Yoon et al., 2010). If surround suppression deficits do indeed

depend on GABA, then our results may point to the unique impairment of a particular sub-type of GABA neurons among SZ and BP patients. The role of GABAergic inhibition during surround suppression is not yet fully understood (Ozeki et al., 2004; Ozeki et al., 2009; Haider et al., 2010). However, recent work indicates that early- and late-stage suppression may involve different sub-types of GABAergic neurons in V1. The activity of Parvalbumin-positive (PV+) neurons appears consistent with early un-tuned suppression, while Somatostatin-positive (SOM+) inhibition more closely matches the later sharply tuned component described above (Ma et al., 2010; Adesnik et al., 2012; Atallah et al., 2012; Nienborg et al., 2013). Thus, our observation of weaker surround suppression across conditions in SZ and BP may suggest a deficit in an early un-tuned suppression mechanism, which may be consistent with impaired PV+ GABAergic functioning. Our results also suggest that the inclusion of BP subjects, as well as multiple stimulus conditions designed to probe the neural mechanisms underlying surround suppression (Nurminen and Angelucci, 2014), may benefit future studies of GABAergic functioning in SZ.

Dakin and colleagues (2005) reported weaker surround suppression in patients with SZ, but normal suppression among a psychiatric control group, compared with healthy controls. Diagnoses varied among the 13 psychiatric control subjects in their study, including bipolar affective disorder as well as personality disorder, post-traumatic stress disorder, and treatment-resistant mood disorders (the number of subjects with each diagnosis was not provided). Studying a larger group of subjects (n = 19) with more homogenous diagnoses allowed us to observe a modest deficit in surround suppression

among BP subjects in the current study. However, reports of impaired visual processing in both SZ and BP are not without precedent; one group found equivalent deficits among SZ and BP subjects in a shine-through Vernier masking task (Chkonia et al., 2012). This result differs from other studies showing normal masking in BP (Goghari and Sponheim, 2008; Sponheim et al., 2012; Jahshan et al., 2014), which may reflect differences in patient group composition and/or task requirements (e.g., Vernier vs. object configuration discrimination). Additionally, in a rapid serial visual presentation task (Jahshan et al., 2014), SZ subjects showed strongly impaired letter identification at intervals expected to evoke an attentional blink effect, while BP subjects showed a more modest impairment (intermediate to SZ and HC). Thus, our observation of a moderate deficit in surround suppression in BP might reflect a shared impairment in visual context processing among patients with psychotic mental disorders, as suggested by some of the reports above (but see also Chen et al., 2005; Kéri et al., 2005).

Previous work has also examined visual processing in patients and their unaffected relatives, in order to assess how a genetic risk for mental illness might contribute to task performance (Kéri et al., 2001; Must et al., 2004; Chkonia et al., 2010; Sponheim et al., 2012; Schallmo et al., 2013). Studies of backward masking have reported impairments to varying degrees among SZrels (Kéri et al., 2001; Must et al., 2004; Chkonia et al., 2010; Sponheim et al., 2012). In contrast, we have previously reported normal performance among SZrels in a visual contour detection task, as well as a normal modulation by surrounding stimulus orientation (Schallmo et al., 2013). A distinction between temporal and spatial masking may explain the discrepancy between

our observation of normal surround suppression among relatives and previously reported impairments in backward masking. Additionally, one study reported normal masking effects among BPrels (Kéri et al., 2001), which is consistent with our report of normal surround suppression in this group. Normal performance in SZrel and BPrel subjects suggests that deficient surround suppression reflects the clinical expression of psychotic disorders, rather than marking genetic liability for such conditions.

Conclusion

We observed weaker visual surround suppression among subjects with SZ versus HC and relatives, while BP subjects showed an intermediate deficit. Deficits among patients did not depend on surrounding stimulus configuration, as suppression was weaker across conditions. Reduced surround suppression was not associated with a genetic risk for SZ or BP, as both groups of relatives exhibited normal performance. While higher IQ correlated with stronger surround suppression, our secondary analysis showed that high-IQ BP and SZ subjects also showed reduced suppression versus HC, and thus results did not appear consistent with a generalized deficit among patients. We conclude that disease processes associated with SZ, and to a lesser extent BP, reduce surround suppression of perceived contrast regardless of center-surround similarity. This deficit is consistent with reduced suppression at an early stage of visual processing such as the LGN or V1, and/or weaker PV+ inhibition. These mechanisms may therefore serve as fruitful targets for future research into the neural underpinnings of these mental disorders.

Chapter 4 :

Abnormal Contextual Modulation of Visual Contour Detection in Patients with Schizophrenia

Authors: Michael-Paul Schallmo, Scott R. Sponheim, Cheryl A. Olman

PLOS ONE (2013), 8(6), e68090.

Summary

Schizophrenia patients demonstrate perceptual deficits consistent with broad dysfunction in visual context processing. These include poor integration of segments forming visual contours, and reduced visual contrast effects (e.g. weaker orientation-dependent surround suppression, ODSS). Background image context can influence contour perception, as stimuli near the contour affect detection accuracy. Because of ODSS, this contextual modulation depends on the relative orientation between the contour and flanking elements, with parallel flankers impairing contour perception. However in schizophrenia, the impact of abnormal ODSS during contour perception is not clear. It is also unknown whether deficient contour perception marks genetic liability for schizophrenia, or is strictly associated with clinical expression of this disorder. We examined contour detection in 25 adults with schizophrenia, 13 unaffected first-degree biological relatives of schizophrenia patients, and 28 healthy controls. Subjects performed a psychophysics experiment designed to quantify the effect of flanker orientation during contour detection. Overall, patients with schizophrenia showed poorer

contour detection performance than relatives or controls. Parallel flankers suppressed and orthogonal flankers enhanced contour detection performance for all groups, but parallel suppression was relatively weaker for schizophrenia patients than healthy controls. Relatives of patients showed equivalent performance with controls. Computational modeling suggested that abnormal contextual modulation in schizophrenia may be explained by suppression that is more broadly tuned for orientation. Abnormal flanker suppression in schizophrenia is consistent with weaker ODSS and/or broader orientation tuning. This work provides the first evidence that such perceptual abnormalities may not be associated with a genetic liability for schizophrenia.

Introduction

In everyday visual perception, objects and paths are defined by visual contours. Contour detection is a perceptual process that is critical for identifying visual edges and boundaries, plays an important role in figure-ground segmentation, and is essential for locating and recognizing objects (for a review see Loffler, 2008). Contours are sometimes composed of individual elements that are spatially separated, for example when one object occludes part of another. When broken contours are encountered during normal vision, attributes or features such as the contrast, spacing, and relative orientation of contour elements, as well as curvature, closure, and contour length strongly influence perception, as demonstrated in psychophysical (Field et al., 1993; Bonneh and Sagi, 1998; Li and Gilbert, 2002), electrophysiological (Li et al., 2006), and neuroimaging experiments (Altmann et al., 2003). These observations are in general agreement with the rules of perceptual organization, such as proximity, continuity and similarity, as

described in Gestalt psychology (Wertheimer, 1938). Patients with schizophrenia perform worse than healthy controls in contour integration paradigms (Silverstein et al., 2000; Parnas et al., 2001; Uhlhaas et al., 2005; Silverstein et al., 2006b; Uhlhaas et al., 2006; Silverstein et al., 2009), but the manner in which stimulus features affect this perceptual deficit is not fully understood.

Not only do the features of a visual contour affect perception, but the context (or background) in which a contour appears also modulates perceptual saliency, an effect commonly referred to as contextual modulation. Orientation-dependent surround suppression (ODSS) is one form of contextual modulation that applies to a broad range of stimuli; the perceptibility of a target is affected by the position and relative orientation of nearby stimuli. Recent psychophysical work in the field of contour perception has shown that parallel flanking elements tend to suppress perception of target contours, while orthogonal flankers cause less suppression, in agreement with ODSS (Dakin and Baruch, 2009; Kingdom and Prins, 2009; Schumacher et al., 2011b; Robol et al., 2012). Extensive investigations of contextual effects during early visual processing have been made among healthy subjects in past decades, and several groups have recently demonstrated weaker surround suppression effects among patients with schizophrenia compared with controls (Dakin et al., 2005; Tadin et al., 2006; Yoon et al., 2009; Tibber et al., 2013; Yang et al., 2013); but see (Chen et al., 2008; Barch et al., 2012).

Both contour integration and surround suppression have been highlighted as examples of well documented visual abnormalities in schizophrenia whose investigation may provide insight into the neural underpinnings of this disorder (Butler et al., 2008).

However, it is not yet known to what extent genetic liability for schizophrenia may contribute to such abnormalities. Further, previous investigations of contour integration deficits in schizophrenia have not specifically examined the role of surrounding stimulus orientation during task performance. Thus, it is not clear how surround suppression deficits in schizophrenia may affect contour perception. In order to better understand the neural mechanism(s) underlying impaired contour detection and abnormal ODSS in this disorder, we examined the performance of patients with schizophrenia, unaffected first-degree biological relatives of schizophrenia patients, and healthy controls during a contour detection paradigm, while manipulating the local orientation context in which target contours appeared. Computational modeling allowed us to separately and quantitatively characterize baseline task performance, the strength of contextual modulation, and its dependence on flanker orientation.

Methods

Summary

Patients with schizophrenia, unaffected first-degree biological relatives of schizophrenia patients, and healthy control subjects were recruited to perform a contour detection task. Subjects detected an open vertical contour within a briefly presented array of Gabor stimuli (Gaussian-enveloped sinusoidal luminance modulation, see Figure 4-1). Target contours were presented either to the right or to the left of fixation and were flanked by Gabors that were parallel, orthogonal or randomly oriented relative to the vertical contour, which defined the stimulus condition. Our group has previously examined contour detection in healthy adults using this paradigm (Schumacher et al.,

2011b). Task performance was quantified in terms of contour detection thresholds corresponding to the level of orientation jitter for which a subject would detect target contours with 79% accuracy.

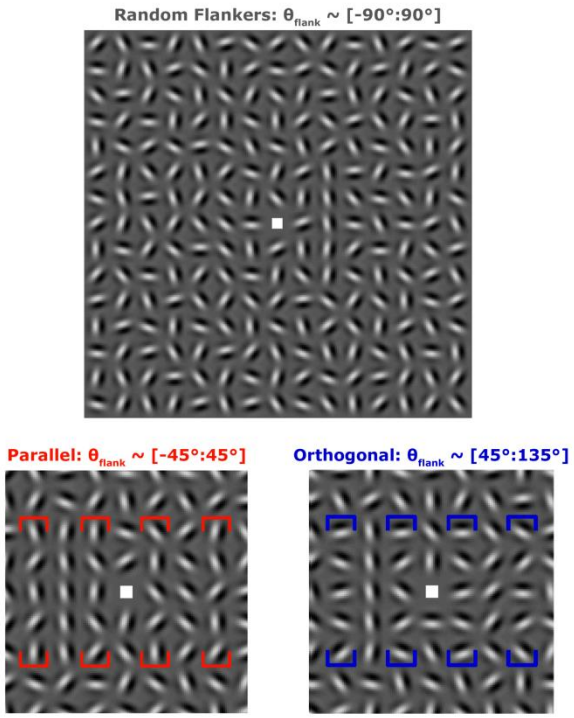

Figure 4-1. Example stimuli.
Top, Random condition. Target contours (composed of 5 Gabors) were presented in a vertical line in the second column to either the right (as shown in top example) or left of fixation. The Gabors horizontally adjacent to possible target positions are termed flankers, and were oriented randomly in this condition. The distribution of flanker orientations is shown at the top of each panel in brackets. Bottom left, zoomed region to show detail of Parallel condition. Average orientation of flankers (four bracketed sets) is parallel to the vertical contour axis. Target contour is presented on the left in both bottom panels. Flankers surrounded both possible target contour locations on every trial. Bottom right, detail of Orthogonal condition. Flankers (bracketed) are on average oriented orthogonal to the vertical target contour.

Participants

Twenty eight outpatients (25 with schizophrenia, 3 with schizoaffective disorder – depressed type), 15 first-degree biological relatives of schizophrenia patients, and 29 healthy controls were recruited through the VA Hospital in Minneapolis, MN.

Participants were excluded according to the following criteria: English as a second language, mental retardation, current alcohol abuse/drug dependence, current or past central nervous system condition, history of head injury with skull fracture or substantial loss of consciousness, history of electroconvulsive therapy, age less than 18 or greater than 60. Healthy controls were absent diagnoses of bipolar disorder and any psychotic disorder in themselves and their first-degree biological relatives.

The Structured Clinical Interview for DSM Disorders and the Psychosis Module of the Diagnostic Interview for Genetic Studies (First, 1997) were completed with each participant, and DSM-IV-TR diagnoses (APA, 2000) were made by a doctoral-level clinical psychologist. All participants had psychiatric functioning assessed using the Brief Psychiatric Rating Scale (BPRS; Overall and Donald, 1962), with controls and relatives additionally completing the Schizotypal Personality Questionnaire (SPQ; Raine, 1991). IQ was estimated from the Wechsler Adult Intelligence Scale (WAIS-III; Jeyakumar et al., 2004). Parental education was assessed among patients and controls using a 7 point scale self-report questionnaire, with 1 corresponding to completing 7^{th} grade or less, and 7 indicating completion of a graduate degree. Mean education score from both parents was taken for each subject. Medication dosages for schizophrenia patients were converted to Chlorpromazine equivalents (in milligrams; Andreasen et al., 2010). Demographic data are presented in Table 4-1. Age, parental education, and SPQ scores were not different between groups. Gender distributions differed, with more males than females recruited among patients. BPRS scores were higher, and years of education were lower for patients and relatives than for controls. Estimated IQ was marginally different between groups,

and tended to be lower among patients than controls. All participants had normal or corrected-to-normal vision.

Ethics statement

Experimental protocols were approved by Institutional Review Boards at the University of Minnesota and Minneapolis VA Medical Center. Subjects gave written informed consent prior to participation, and were paid $15 per hour. The researcher conducting the consent process provided a description of the protocol, outlined the potential risks and benefits of participation, and explained that the decision to participate had no bearing on services obtained at the VA Medical Center, including psychiatric treatment for patients, as stated in the consent form. Individuals who declined to participate in the study were not disadvantaged in any way.

Table 4-1. Subject group demographics.

Index	**Scz** (n = 25)	**Rel** (n = 13)	**Cont** (n = 28)	**Statistics**
Age (years)	41.8 (11.9)	40.1 (14.7)	45.1 (11.6)	$F_{(2,63)} = 0.88$, $p = 0.42$
Gender (n) [1]				$X^2_{(2)} = 8.24$, $p = 0.02$
Female	4	7	14	
Male	21	6	14	
Education (years) [2]	13.5 (1.5)	13.2 (1.4)	15.2 (1.8)	$F_{(2,63)} = 9.83$, $p < 0.01$
Estimated IQ [3] (from WAIS-III)	97.8 (17.6)	107 (17.2)	109 (12.2)	$F_{(2,57)} = 3.15$, $p = 0.05$
Parental Education [a]	4.8 (1.2)	NA	5.0 (1.12)	$F_{(1,51)} = 0.48$, $p = 0.49$
Overall Symptomatology [4] (BPRS Total Score)	42.7 (13.1)	31.9 (6.4)	27.6 (4.02)	$F_{(2,61)} = 18.5$, $p < 0.01$
Schizotypal Characteristics (SPQ Total Score)	NA	15.5 (13.9)	9.7 (6.52)	$F_{(1,29)} = 2.61$, $p = 0.12$
CPZ Equivalents [b]	270 (219)	NA	NA	NA

All data are presented as Mean (Standard Deviation), unless otherwise noted.
Cont = healthy control group, Rel = first-degree relative group, Scz = schizophrenia patient group. WAIS-III – Wechsler Adult Intelligence Scale, 3rd Edition. BPRS = 24-item Brief Psychiatric Rating Scale. SPQ = Schizotypal Personality Questionnaire. NA = not applicable.
[a] Parental education was assessed using a self-report questionnaire on a 7 point rating scale (see Methods).
[b] Medication dosages were calculated in Chlorpromazine equivalents (mg).
[1] There was a marginally significant difference in gender distribution between patients and healthy controls following Yates's and Bonferroni corrections, $X^2_{(1)} = 5.37$, $p = 0.06$.
[2] Education was significantly higher among the healthy control group compared with both patients and first-degree relatives, Tukey's HSD, $p < 0.05$.
[3] There was a marginally significant difference between the Estimated IQ scores for patients and healthy controls, Tukey's HSD, $p = 0.05$.
[4] BPRS scores were significantly lower among the healthy control group compared with both patients and first-degree relatives, Tukey's HSD, $p < 0.05$.
Estimated IQ data were not obtained for 6 healthy controls subjects. One first-degree relative did not report parental education. One healthy control and one first-degree relative did not complete the BPRS. Eight healthy controls and two first-degree relatives did not complete the SPQ.

Stimuli

Stimuli were presented using MATLAB (The MathWorks) and Psychtoolbox (Brainard, 1997; Pelli, 1997) software on a MacMini running OSX. Images were displayed on a Dell 19" monitor that subtended 35.1 x 26.7 degrees of visual angle at a viewing distance of 61 cm. Monitor color look-up table was linearized using custom software. Stimuli consisted of Gabor patches in grids of 15 x 15 elements. Grids subtended 12°. Vertical target contours comprised five aligned Gabors of the same spatial phase located at 1.6° eccentricity to the left or right of the central fixation square. Each Gabor consisted of a 2 cycles per degree sine wave grating modulated by a Gaussian envelope ($\sigma = 0.17°$), spaced 0.8° from one another (i.e., 1.6λ separation, where λ is the wavelength of the sine wave grating). Spacing, carrier frequency and eccentricity were selected to maximize flanker orientation effects based our previous work (Schumacher et al., 2011b). Gabors were presented at 80% contrast. Background was set to mean gray.

Orientation of non-target, non-flanker Gabors was random, but differed by at least 30° between cardinal neighbors to prevent perception of an unintended contour.

Contour detection thresholds were measured for three conditions. In the Random condition, Gabors immediately to the right and left (termed flankers) of the contour were randomly oriented (Figure 4-1, top). In the Parallel and Orthogonal conditions, flanker orientation was drawn from a uniform distribution with ± 45° range centered on 0° or 90° relative to the vertical contour, respectively (flankers bracketed in Figure 4-1, bottom). Note that the orientation of flankers adjacent to both possible target positions (left and right) was drawn from the flanker distribution, regardless of target location on a given trial. This was done to prevent flanker orientation from providing a cue for target detection.

Procedure

Subjects were instructed to use their peripheral vision to detect a contour either to the right or to the left of fixation, and to press the corresponding arrow key. Task difficulty was controlled by varying orientation jitter within the contour. Relative orientation of contour elements was adjusted in steps of 4.5° of jitter (range 0 – 45°). Jitter increased after three consecutive correct responses, and decreased after one incorrect response. This 3-up 1-down staircase converges on a contour detection threshold at the jitter level for which targets are detected with 79% accuracy (Garcia-Perez, 1998). The task was organized into blocks of 30 trials. Flanker orientation was held constant within blocks. Subjects completed at least 3 blocks per condition (9 total). The order of blocks was pseudo-randomized.

At trial onset, the fixation mark appeared for 500 msec. Stimuli were then presented for 150 msec. Response time was not limited. Feedback was given for 100 msec after each response. The fixation mark turned green after correct or red after incorrect responses, then disappeared for 500 msec. Total minimum inter-stimulus interval was 1.1 sec. At next trial onset, the fixation mark (and subsequent stimulus array) was randomly moved within 0.5° of the center of the screen. This eliminated the possibility of successfully performing the task by fixating on potential target positions. Fixation and target positions never overlapped in sequential trials. Task performance was monitored by research staff. Reaction times (RTs) were measured for each trial. Median RTs within blocks were compared between groups in a repeated measures analysis of variance, with subjects nested within groups (abbreviated ANOVA in Results). RTs were not different between groups ($F_{(2,64)} = 0.89$, $p = 0.42$). Median RT across subjects was 633 msec.

Prior to the beginning of main experiment, subjects saw three example stimuli sequentially to ensure task comprehension. In these examples, jitter increased from 0° to 13.5°. Subjects next practiced the task before data collection. Practice consisted of at least two sets of 8 trials, continuing until subjects achieved > 80% accuracy. Contour jitter during the two practice sessions was 0° and 4.5°, respectively. Flanker orientation during practice was random.

Analysis

Contour detection thresholds were obtained for each block of 30 trials by taking the mean jitter level of the last 3 trials in each block. Thresholds were not calculated if

the jitter value was 0° for more than 3 of the last 5 trials in a block, as this indicated performance at floor level. Thresholds were also not calculated if the standard deviation of the jitter values during the last 5 trials was greater than 3.5°, because this indicated unstable performance at the end of the block, which would produce an unreliable threshold estimate. Of 765 runs in all subjects, 39 thresholds were not estimated due to floor performance, and 105 were not estimated due to poor convergence. The distributions of excluded runs did not differ between groups ($X^2_{(2)}$ values < 4.44, p values > 0.10). Subjects were excluded from further analyses if they had fewer than 5 total threshold estimates, or zero thresholds in any condition. Data from 3 patients with schizophrenia, 2 relatives of schizophrenia patients, and 1 healthy control were excluded in this way. The observed pattern of results was not altered by data exclusion. Data from 25 schizophrenia patients, 13 relatives, and 28 controls were included in the final analyses. Contextual modulation indices were calculated for Parallel and Orthogonal blocks for each subject by taking contour detection thresholds and subtracting the subject's mean Random condition threshold. When appropriate, p values were corrected for multiple comparisons using Tukey's Honestly Significant Difference (HSD) or False Discovery Rate (FDR) corrections.

Computational modeling

The following model was used to characterize the dependence of task performance on flanker orientation:

$$T = T_0 + c_s \mathrm{N}_s(\theta_{rel} | 0°, \sigma_s^2)$$

Equation 4-1

where T is the observer's contour detection threshold, and T_0 sets the performance baseline. The term c_s scales the amplitude of flanker suppression, which is defined by N_s, a circular normal function:

$$\mathrm{N}_s(\theta_{rel} | \mu, \sigma_s^2) = e^{\frac{\cos(\theta_{rel} - \mu) - 1}{\sigma_s^2}}$$

Equation 4-2

Using a mean (μ) of 0°, its magnitude is a function of average flanker orientation relative to the contour (θ_{rel} = 0, 45°, or 90°), and its orientation tuning width is set by σ_s. Contour detection thresholds from all three flanker conditions for schizophrenia patients and healthy controls were fit with this model using MATLAB's *lsqcurvefit* function. T_0 was constrained within the interquartile range of patient and control Orthogonal thresholds, c_s was constrained between 0 and the (negative) upper limit of T_0, and σ_s between 0 and 360°. Statistical significance for parameter differences between groups was assessed using a bootstrap procedure, resampling subject data within groups with replacement across 2000 iterations.

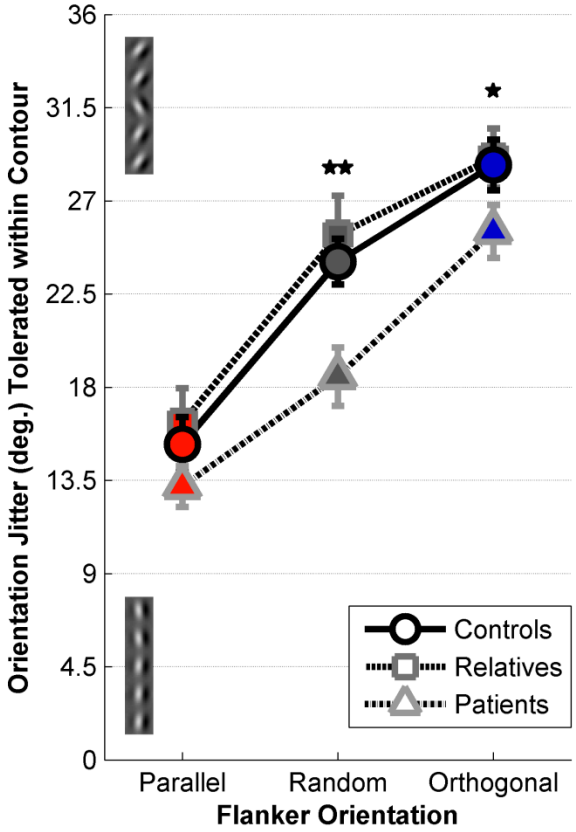

Figure 4-2. Contour detection thresholds.
Mean contour detection thresholds are plotted for 28 healthy controls (circles), 13 first-degree relatives (squares), and 25 patients with schizophrenia (triangles) for the Parallel, Random, and Orthogonal conditions. Example contours with 4.5° jitter (bottom) and 31.5° jitter (top) are shown along the y-axis. Error bars are S.E.M. Double asterisk indicates significant differences in Random condition thresholds between schizophrenia patients and both healthy controls and first-degree relatives, single asterisk indicates a significant difference in Orthogonal condition thresholds between patients and relatives, corrected for multiple comparisons via Tukey's HSD, $p < 0.05$.

Results

Contour detection performance

Contour detection thresholds were examined across three flanker orientation conditions (Parallel, Random, and Orthogonal) and between subject groups (schizophrenia patients, first-degree relatives, and healthy controls). Higher thresholds

indicated more tolerance for orientation jitter within the contour, and thus better contour detection performance. We observed a significant main effect of condition (ANOVA, $F_{(2,63)} = 145$, $p < 0.001$); contour detection performance was worst in the presence of parallel flankers and best in the presence of orthogonal flankers (Figure 4-2). This is consistent with previous reports (Dakin and Baruch, 2009; Schumacher et al., 2011b; Robol et al., 2012). We also observed a significant main effect of group ($F_{(2,63)} = 4.49$, $p = 0.015$), with lower contour detection performance overall for patients than for healthy controls and first-degree relatives. No significant interaction between group and condition was observed ($F_{(4,126)} = 1.76$, $p = 0.140$).

Following up on the significant main effect of group, we tested for group differences on each condition. Patients performed significantly worse than controls and relatives in the Random condition (Tukey's HSD, p values < 0.01, Cohen's $d = 1.12$), significantly worse than relatives in the Orthogonal condition (Tukey's HSD, $p = 0.041$, Cohen's $d = 0.68$), and showed a trend toward poorer Orthogonal performance versus controls that did not survive correction for multiple comparisons (uncorrected $p = 0.006$, Cohen's $d = 0.50$). Trends toward poorer contour detection performance among patients in the Parallel condition also did not survive multiple comparisons correction (uncorrected p values < 0.035, Cohen's d values > 0.40). Performance did not differ significantly between controls and relatives in any condition.

To explore whether demographic factors were associated with task performance, correlations were examined between contour detection thresholds and demographic values across all groups. We observed significant correlations between both Random and

Orthogonal condition thresholds and estimated IQ scores ($r_{(58)}$ = 0.54 and 0.49, FDR corrected p values < 0.001 and 0.002, respectively). Within groups, there were significant correlations between estimated IQ and Random / Orthogonal thresholds among schizophrenia patients ($r_{(23)}$ = 0.70 and 0.68, FDR corrected p values < 0.008 and 0.014, respectively), but not for controls or relatives (uncorrected p values > 0.306). Other demographic factors (education, CPZ equivalents, BPRS and SPQ scores) were not significantly correlated with contour detection thresholds (FDR corrected p values > 0.441). This analysis indicated that baseline task performance may depend in part on IQ score; subsequent analyses therefore focused on effects of context within individuals, since performance differences between flanker conditions should not be confounded by an overall effect of IQ score.

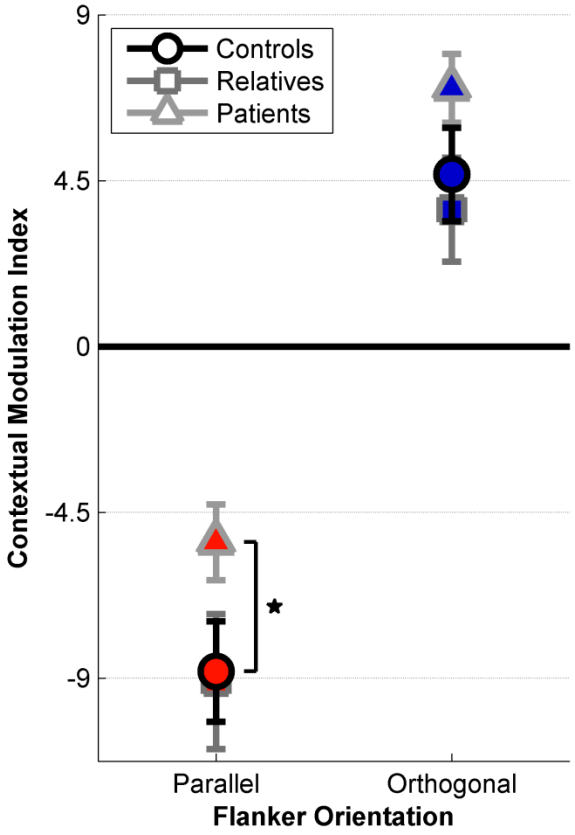

Figure 4-3. Contextual modulation indices.
Mean indices are plotted for 28 healthy controls (circles), 13 first-degree relatives (squares), and 25 patients with schizophrenia (triangles) in the Parallel and Orthogonal conditions. Negative indices indicate conditions where contour detection was suppressed relative to the Random condition, whereas positive indices indicate enhanced contour perception. Asterisk indicates a significant difference between schizophrenia patients and healthy controls, corrected for multiple comparisons via Tukey's HSD, $p < 0.05$. Error bars are S.E.M.

Contextual modulation

As patients with schizophrenia show diminished ODSS effects (Yoon et al., 2009), we predicted that the effect of flanker orientation on contour detection performance would be relatively weaker among patients. In order to test this hypothesis, we calculated Parallel and Orthogonal contextual modulation indices for all subjects (see Figure 4-3). Indices were obtained by subtracting the Random condition threshold from

those obtained in the Parallel and Orthogonal conditions. This metric quantified the relative effect of flanker orientation in terms of increased or decreased tolerance to orientation jitter within the contour, irrespective of overall task performance. Patients showed abnormal contextual modulation compared with first-degree biological relatives and healthy controls (ANOVA, $F_{(2,63)} = 3.15$, $p = 0.049$).

Post-hoc analyses revealed that in the Parallel condition, contextual modulation indices were significantly weaker among patients than controls (Tukey's HSD, $p = 0.017$, Cohen's $d = 0.68$). This indicated that patients with schizophrenia could tolerate relatively more orientation jitter within the target contour in the Parallel condition, and thus performed *better* than the controls in the presence of suppressive parallel flankers, relative to the Random condition. There were trends toward higher Orthogonal indices among patients versus controls (uncorrected $p = 0.044$, Cohen's $d = 0.47$), and for higher indices among patients versus relatives in both conditions (uncorrected p values < 0.02, Cohen's d values > 0.70); however, these did not survive correction for multiple comparisons. Contextual modulation indices did not differ between controls and relatives (uncorrected p values > 0.250, Cohen's d values < 0.19). In addition, contextual modulation indices were not significantly correlated with demographic factors (estimated IQ, education, CPZ equivalents, BPRS and SPQ scores, FDR corrected p values > 0.321).

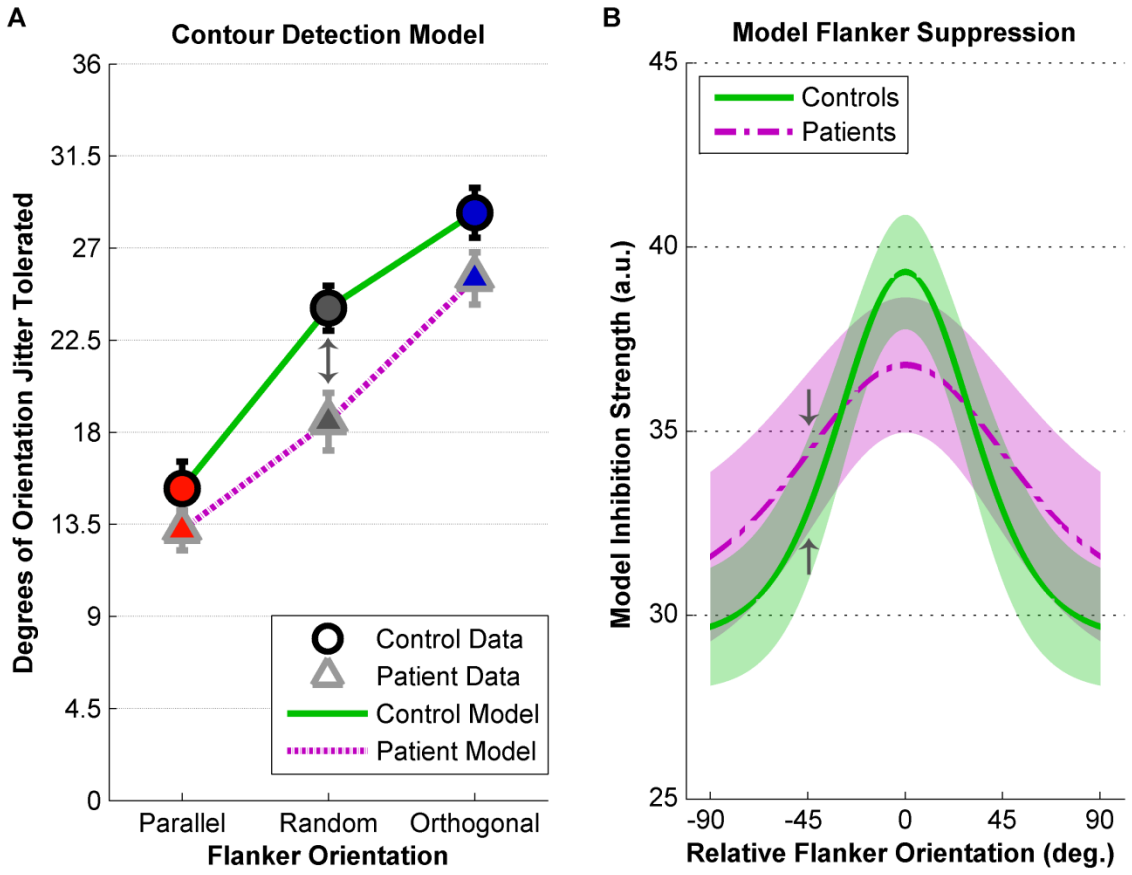

Figure 4-4. Computational modeling.
Computational model predications based on parameters from Table 4-2 for 28 control subjects (solid lines) and 25 schizophrenia patients (dashed lines). A) Equation 4-1 was fit to contour detection task data in all three flanker conditions from healthy controls (circles) and patients with schizophrenia (triangles). Plotted thresholds are identical to those in Figure 4-2. Error bars are S.E.M. B) Bootstrapped estimates of T_0, c_s and σ_s were used to calculate flanker suppression orientation tuning distributions (in arbitrary units) for the control and patient groups. Lines plot the mean bootstrapped tuning curves for patients and controls. Shaded regions illustrate 1 standard deviation of the bootstrapped distributions for each group. Arrows indicate corresponding positions in both panels.

Computational modeling

We fit the contour detection thresholds in all three flanker conditions from patient and control groups with a computational model that allowed us to quantify the effect of relative orientation of flanking elements on contour detection performance (Equation 4-1,

Methods). Figure 4-4A shows control and patient contour detection thresholds (same data as in Figure 4-2) with the model predictions from the fit parameters shown in Table 4-2.

Table 4-2. Computational model parameters.
Parameters for computational modeling of contour detection task performance. Parameters were fit to group contour detection thresholds from all three flanker conditions using Equation 4-1 (see Methods). Values shown are the parameters best fit to the group data (values in parentheses indicate bootstrapped 95% confidence intervals).

Parameter:	T_0	c_s	σ_s
Values for control subjects:	29.2 (26.6 : 31.5)	-13.9 (-16.7 : -11.5)	0.54 (0.41 : 0.71)
Values for schizophrenia patients:	30.4 (26.0 : 31.5)	-17.2 (-20.0 : -13.0)	0.89 (0.64 : 1.07)

Bootstrap analyses showed that model parameters T_0 (baseline contour detection performance) and c_s (overall magnitude of flanker suppression) were not significantly different between groups (Z scores = 0.67 and 1.34, FDR corrected p values = 0.75 and 0.18, respectively). Values of σ_s, however, differed between groups (Z = 3.29, FDR corrected $p < 0.002$), with the model predicting significantly wider orientation tuning of flanker suppression for patients versus controls. Bootstrapped flanker suppression orientation tuning functions for both groups are shown in Figure 4-4B. These illustrate that for patients, more broadly tuned suppression (vs. controls) fit the data well. In summary, computational modeling of experimental data suggests that flanker suppression, which impairs contour detection accuracy, may be more broadly tuned for orientation among patients with schizophrenia.

Discussion

We observed impaired contour detection performance among patients with schizophrenia compared with healthy controls and first-degree biological relatives of patients. We also found abnormal contextual modulation among patients, with parallel flankers causing less of a performance decrement (relative to random) for patients than for controls. One explanation for our pattern of results is that schizophrenia leads to an overall impairment in contour integration, in agreement with previous reports (Silverstein et al., 2000; Parnas et al., 2001; Must et al., 2004; Kéri et al., 2005; Uhlhaas et al., 2005; Silverstein et al., 2006b; Uhlhaas et al., 2006; Kéri et al., 2009; Silverstein et al., 2009; Keane et al., 2012; Silverstein et al., 2012). This is supported by the group difference observed in contour detection thresholds (but no significant group by condition interaction), with patients showing poorest group mean performance in all three flanker conditions. An overall deficit in contour perception may be somewhat offset in the Parallel condition by diminished ODSS in schizophrenia (Yoon et al., 2009), as evidenced by reduced Parallel contextual modulation found in post-hoc analyses. These competing effects may have limited the power of our study to detect a group by orientation context interaction, as observed previously (Yoon et al., 2009).

Alternatively, our results may be consistent with less selective orientation detectors in early visual cortex (Rokem et al., 2011), which could give rise to broader tuning of ODSS in schizophrenia. For nearby stimuli within a wide range of flanker orientations, broader ODSS could impair the perceptual salience of a contour during feature integration. We observed the greatest difference in contour detection performance

between patients and controls with randomly oriented flankers (which on average are oriented 45° relative to the contour), consistent with the large difference in suppression between groups demonstrated in our model at this flanker orientation (e.g. arrows, Figure 4-4). Thus, our model characterized the pattern of results in terms of broader orientation tuned suppression without significant differences in overall performance or suppression strength. Broader orientation tuning among patients should produce weaker Parallel contextual modulation, but larger Orthogonal modulation compared with controls, indicating greater release from flanker suppression between Random and Orthogonal conditions in schizophrenia. Consistent with this proposal, we observed an overall group difference in contextual modulation (but no significant group by condition interaction), weaker Parallel suppression, and a trend toward greater Orthogonal enhancement for patients. Similarly broad tuning has been reported for basic visual responses among schizophrenia patients (Rokem et al., 2011), and others have proposed that broader tuning for stimulus features may underlie abnormal visual masking in schizophrenia (Green et al., 2011).

Although both poorer contour integration with weak flanker suppression and broader orientation tuning with intact contour integration may account for the results we observed in schizophrenia, it is not straightforward to distinguish between these explanations in the current paradigm. One method for teasing apart such proposals would be to examine contextual modulation of contour perception as a function of spacing between stimulus elements. As element separation increases, overall contour detection performance should decrease, but flanker effects should decrease more rapidly, resulting

in weak or absent contextual modulation at higher spacing (Schumacher et al., 2011b). A recent report examined contour integration in schizophrenia at two spacing levels (Keane et al., 2012). They found evidence of a contour integration deficit among patients at target Gabor separations of 0.7° and 1.4° (relative spacing was 3.5λ and 7λ, approximately 2 - 4 times the contour spacing in the current study). While their study did not manipulate flanker orientation, they did observe a consistent performance deficit across a range of spacing over which our previous work (Schumacher et al., 2011b) indicates that flanker effects should change dramatically. Their results therefore suggest that broader orientation tuning of flanker suppression cannot fully account for the contour perception deficits observed in the current study among schizophrenia patients. Others have recently reported weaker suppression of contour perception by parallel flankers and poorer orientation discrimination in patients with schizophrenia vs. controls, and interpreted their results within the framework of impaired visual crowding (Robol et al., 2013).

The current study is the first to investigate whether genetic factors are associated with abnormal contour detection in schizophrenia by examining the performance of patients' first-degree biological relatives. We observed no significant difference between healthy controls and relatives in either contour detection performance or in contextual modulation. From this, we conclude that abnormal contour perception likely has a closer association with the pathophysiology of schizophrenia, rather than with a genetic liability for this disorder. However, the number of relatives included (n = 13) is somewhat low for a psychophysical study in a clinical population, and was smaller than that of our other

groups, which may have limited the current study's power. This smaller sample size may increase the possibility of Type II errors, if for example a large proportion of recruited relatives happen by chance not to be carriers of a genetic variant that influences contour perception, if such genetic factors were to exist. While we find that abnormalities in contour integration and flanker suppression may not prove useful as endophenotypes in schizophrenia, they may instead serve as markers of the current state of neurobiological functioning within the visual system.

Previous work has touched on the role of genetics in other early visual processing tasks in schizophrenia. Our results showing normal behavioral performance among relatives of schizophrenia patients agree with the findings of Silverstein and colleagues (2006a), who observed that subjects at high risk for developing schizophrenia tended to perform as well as healthy controls in a perceptual organization task. Our findings also agree with previous work showing that symptom remission in patients with disorganized schizophrenia (but not in other psychiatric patients) coincided with improved contour integration (Uhlhaas et al., 2005). These reports offered preliminary evidence that visual integration deficits in schizophrenia have an association with disease processes, but not genetic factors. By examining contour detection performance among unaffected first-degree biological relatives of schizophrenia patients, we have provided a stronger test of this hypothesis.

Our results agree in part with the findings of Uhlhaas and colleagues (2004), who observed poorer contour integration and weaker context modulation of perceived size among non-clinical schizotypal subjects with disordered thoughts. While we did not

assess thought disorders in the current study, we found no association between clinical rating scale scores (BPRS and SPQ) and task performance, which may be related to the fact that the recruited outpatients were not highly symptomatic. In contrast to our current results, others have found abnormal backward masking in schizophrenia vs. controls during Vernier discrimination, but no difference between groups in the effect of orientation context (Schütze et al., 2007; Roinishvili et al., 2008). Previous work has also shown impairments among unaffected relatives of schizophrenia patients during visual backward masking (Sponheim et al., 2012). It is possible that genetic factors have a stronger influence on the temporal dynamics of early visual processing compared with static pattern vision.

Our task was designed to examine whether contour detection specifically is impaired in schizophrenia. We asked subjects to detect open vertical contours rather than closed figures of a particular shape, thereby mitigating the role of shape representation in task performance. Previous reports of contour integration deficits in schizophrenia have required subjects to locate closed contours at variable positions within the stimulus array (Silverstein et al., 2000; Parnas et al., 2001; Uhlhaas et al., 2005; Silverstein et al., 2006b; Uhlhaas et al., 2006), or to discriminate contour shape configurations (Silverstein et al., 2009; Keane et al., 2012; Silverstein et al., 2012). Such tasks required subjects to identify contours whose features (position within an array, global orientation, and local curvature) varied between trials. Performance within these paradigms relies on a subject's ability to distinguish the shape of the figure formed by the closed contour. A recent report suggested that perceptual integration deficits in schizophrenia might depend more on

impaired shape representation than on abnormal contour detection (Keane et al., 2012). The current study did not require visual search or shape discrimination during task performance, yet we nonetheless observed poorer contour detection performance among patients in the Random condition (the one most directly comparable to previous studies). Our results therefore suggest that abnormal contour detection in schizophrenia is a specific perceptual abnormality that is distinct from shape representation impairments that may additionally exist in this disorder.

In the current paradigm, we sought to exclude the role of non-specific deficits among schizophrenia patients. A recent report suggested attentional factors may account for the weak contrast-contrast effect (Barch et al., 2012) observed when schizophrenia patients reported the perceived contrast of stimuli with and without surrounding context (Dakin et al., 2005); but see (Tibber et al., 2013). Our study sought to rule out such potential confounds in the following ways: (1) there is no categorical difference between our stimulus conditions based on the absence of surrounding stimuli (Dakin et al., 2005; Barch et al., 2012), so equal effort/attention is required in all conditions; (2) we equated difficulty across flanker conditions using a staircase method to manipulate contour jitter, so all subjects performed at the same level (79% correct) in all conditions; (3) we used contextual modulation indices as dependent variables, making the analyses robust against between groups differences in attention or IQ that might impact overall performance. Indeed, we did not observe significant correlations between contextual modulation indices and estimated IQ, despite such correlations being observed between IQ and contour detection thresholds in the Random and Orthogonal conditions. Task

performance among patients was also relatively better than for healthy controls in the presence of parallel flankers, which further argues against the notion that a generalized deficit could account for this result. Others have previously demonstrated that perceptual integration abnormalities in schizophrenia exist independent of a generalized deficit, using tasks in which poorer integration leads to a performance advantage among patients (Place and Gilmore, 1980; Silverstein and Keane, 2011). Finally, previous reports have demonstrated normal fixation in schizophrenia (Kissler and Clementz, 1998; Gooding et al., 2000), and fixational instability would not affect contextual modulation.

Our findings relate to several outstanding questions that merit further investigation. First, the physiological correlates of abnormal flanker suppression during contour detection in schizophrenia are not yet clear. Through the use of functional MRI (fMRI), abnormal early visual cortical responses during contour integration have been observed among patients (Silverstein et al., 2009), suggesting that schizophrenia leads to disruptions in contour perception at the earliest stages of cortical processing. Further, diminished surround suppression effects have been found to correlate with lower γ-aminobutyric acid (GABA) concentrations in schizophrenia, as measured by magnetic resonance spectroscopy (MRS; Yoon et al., 2010), lending support to the hypothesis that schizophrenia is related to disruptions in GABAergic inhibition (Lewis et al., 2005). Future investigations employing spatially localized fMRI and GABA MRS in visual cortex could help elucidate the neural mechanisms underlying these perceptual abnormalities.

The relationship between abnormal contextual modulation and other visual deficits in schizophrenia also requires further investigation. Patients with schizophrenia have trouble organizing perceptual information, and some experience visual hallucinations (Place and Gilmore, 1980; Silverstein and Keane, 2011). The Gestalt principles of proximity and similarity (Wertheimer, 1938) agree generally with the spatial and orientation specificity of ODSS, which leads us to speculate that abnormal surround suppression may contribute to poorer Gestalt perception in schizophrenia, thereby impairing perceptual grouping. In addition, abnormal electrophysiological activity within visual cortex has been observed in schizophrenia during illusory contour/Gestalt perception (Spencer et al., 2003; Spencer et al., 2004; Foxe et al., 2005). One study found that occipital signal abnormalities were associated with visual hallucinations (Spencer et al., 2004). Abnormal neural synchrony within occipital cortex may therefore be a hallmark of impaired visual feature-binding, which could contribute to both poor contour integration and visual hallucinations in schizophrenia.

Conclusion

The current study has affirmed previous reports of abnormal contour perception among patients with schizophrenia (Silverstein et al., 2000; Parnas et al., 2001; Uhlhaas et al., 2005; Silverstein et al., 2006b; Uhlhaas et al., 2006; Silverstein et al., 2009; Keane et al., 2012; Silverstein et al., 2012), even with open vertical target contours presented at fixed spatial positions. In addition, we have found that patients are relatively less impaired by the presence of parallel flanking stimuli during contour detection, compared with healthy adults. This agrees with weaker perceptual surround suppression effects

reported in schizophrenia (Dakin et al., 2005; Tadin et al., 2006; Yoon et al., 2009; Tibber et al., 2013; Yang et al., 2013). Computational modeling of patient data showed that our results are consistent with broader orientation tuning in schizophrenia (Rokem et al., 2011). We conclude that schizophrenia leads to deficits in contour detection that are consistent with poorer overall integration and weaker parallel flanker suppression, or with broader tuning for visual stimulus orientation. We did not observe any difference between healthy controls and first-degree biological relatives of schizophrenia patients in contour detection performance or in contextual modulation. These visual processing abnormalities are concomitant with the pathophysiology of schizophrenia, but may not be associated with a genetic liability for this disorder.

Bibliography

Adesnik H, Bruns W, Taniguchi H, Huang ZJ, Scanziani M (2012) A neural circuit for spatial summation in visual cortex. Nature 490:226-231.

Adriany G, Waks M, Tramm B, Schillak S, Yacoub E, DeMartino F, Van de Moortele P-F, Naselaris T, Olman CA, Vaughan JT, Ugurbil K (2012) An open faced 4 ch. loop transmit / 16 ch. receive array coil for HiRes fMRI at 7 Tesla. In: 20th Annual Meeting of the International Society for Magnetic Resonance in Medicine. Melbourne, Australia.

Albrecht DG, Hamilton DB (1982) Striate cortex of monkey and cat: Contrast response function. Journal of Neurophysiology 48:217-237.

Altmann C, Bülthoff H, Kourtzi Z (2003) Perceptual organization of local elements into global shapes in the human visual cortex. Current Biology 13:342-349.

Andreasen NC (1982) Negative symptoms in schizophrenia: Definition and reliability. Archives of General Psychiatry 39:784-788.

Andreasen NC (1984) Scale for the assessment of positive symptoms. In. Iowa City, IA: University of Iowa.

Andreasen NC, Pressler M, Nopoulos P, Miller D, Ho B-C (2010) Antipsychotic dose equivalents and dose-years: A standardized method for comparing exposure to different drugs. Biological Psychiatry 65:255-262.

Angelucci A, Bullier J (2003) Reaching beyond the classical receptive field of V1 neurons: Horizontal or feedback axons? Journal of Physiology - Paris 97:141-154.

Angelucci A, Bressloff PC (2006) Contribution of feedforward, lateral, and feedback connections to the classical receptive field center and extra-classical receptive field surround of primate V1 neurons. In: Progress in Brain Research (Martinez-Conde M, Martinez, Alonso, & Tse, ed), pp 93-120.

Angelucci A, Levitt JB, Walton EJS, Hupe J-M, Bullier J, Lund JS (2002) Circuits for local and global signal integration in primary visual cortex. The Journal of Neuroscience 22:8633-8646.

APA (2000) Diagnostic and statistical manual of mental disorders: DSM-IV-TR: American Psychiatric Publishing, Inc.

Atallah BV, Bruns W, Carandini M, Scanziani M (2012) Parvalbumin-Expressing Interneurons Linearly Transform Cortical Responses to Visual Stimuli. Neuron 73:159-170.

Bair W, Cavanaugh JR, Movshon JA (2003) Time course and time-distance relationships for surround suppression in macaque V1 neurons. The Journal of Neuroscience 23:7690-7701.

Barch DM, Carter CS, Dakin SC, Gold J, Luck SJ, MacDonald AW, Ragland JD, Silverstein S, Strauss ME (2012) The clinical translation of a measure of gain control: The contrast-contrast effect task. Schizophrenia Bulletin 38:135-143.

Bauer R, Heinze S (2002) Contour integration in striate cortex. Experimental Brain Research 147:145-152.

Bonneh Y, Sagi D (1998) Effects of spatial configuration on contrast detection. Vision Research 38:3541-3553.
Bouvier SE, Engel SA (2011) Delayed effects of attention in visual cortex as measured with fMRI. NeuroImage 57:1177-1183.
Boynton GM, Engel SA, Glover GH, Heeger DJ (1996) Linear systems analysis of functional magnetic resonance imaging in human V1. The journal of neuroscience 16:4207-4221.
Boynton GM, Demb JB, Glover GH, Heeger DJ (1999) Neuronal basis of contrast discrimination. Vision Research 39:257-269.
Brainard D (1997) The Psychophysics Toolbox. Spatial Vision 10:433-436.
Brefczynski JA, DeYoe EA (1999) A physiological correlate of the'spotlight'of visual attention. Nature neuroscience 2:370-374.
Bressler DW, Fortenbaugh FC, Robertson LC, Silver MA (2013) Visual spatial attention enhances the amplitude of positive and negative fMRI responses to visual stimulation in an eccentricity-dependent manner. Vision Research 85:104-112.
Buracas GT, Boynton GM (2007) The effect of spatial attention on contrast response functions in human visual cortex. Journal of Neuroscience 27:93-97.
Butler PD, Silverstein S, Dakin SC (2008) Visual perception and its impairment in schizophrenia. Biological Psychiatry 64:40-47.
Butler PD, Abeles IY, Silverstein SM, Dias EC, Weiskopf NG, Calderone DJ, Sehatpour P (2013) An event-related potential examination of contour integration deficits in schizophrenia. Frontiers in Psychology 4:132.
Butler PD, Zemon V, Schecter I, Saperstein AM, Hoptman MJ, Lim KO, Revheim N, Silipo G, Javitt DC (2005) Early-stage visual processing and cortical amplification deficits in schizophrenia. Archives of General Psychiatry 62:495-504.
Cai Y, Zhou T, Chen L (2008) Effects of binocular suppression on surround suppression. Journal of Vision 8:9.
Cannon MW, Fullenkamp SC (1991) Spatial interactions in apparent contrast: inhibitory effects among grating patterns of different spatial frequencies, spatial positions and orientations. Vision research 31:1985-1998.
Carandini M, Heeger DJ (2012) Normalization as a canonical neural computation. Nature Reviews Neuroscience 13:51-62.
Cavanaugh JR, Bair W, Movshon JA (2002) Selectivity and spatial distribution of signals from the receptive field surround in macaque V1 neurons. Journal of Neurophysiology 88:2547-2556.
Chen C-C (2014) Partitioning two components of BOLD activation suppression in flanker effects. Frontiers in Neuroscience 8:149.
Chen C-C, Kasamatsu T, Polat U, Norcia AM (2001) Contrast response characteristics of long-range lateral interactions in cat striate cortex. NeuroReport 12:655-661.
Chen Y, Bidwell LC, Holzman PS (2005) Visual motion integration in schizophrenia patients, their first-degree relatives, and patients with bipolar disorder. Schizophrenia Research 74:271-281.

Chen Y, Norton D, Ongur D (2008) Altered center-surround motion inhibition in schizophrenia. Biological Psychiatry 64:74-77.
Chkonia E, Roinishvili M, Makhatadze N, Tsverava L, Stroux A, Neumann K, Herzog MH, Brand A (2010) The shine-through masking paradigm is a potential endophenotype of schizophrenia. PLOS ONE 5:e14268.
Chkonia E, Roinishvili M, Reichard L, Wurch W, Puhlmann H, Grimsen C, Herzog MH, Brand A (2012) Patients with functional psychoses show similar visual backward masking deficits. Psychiatry Research 198:235-240.
Chouinard PA, Noulty WA, Sperandio I, Landry O (2013) Global processing during the Müller-Lyer illusion is distinctively affected by the degree of autistic traits in the typical population. Experimental Brain Research 230:219-231.
Cox RW (1996) AFNI: software for analysis and visualization of functional magnetic resonance neuroimages. Computers and Biomedical research 29:162-173.
Cox RW, Jesmanowicz A (1999) Real-time 3D image registration for functional MRI. Magnetic Resonance in Medicine 42:1014-1018.
Crook JM, Engelmann R, Lowel S (2002) GABA-inactivation attenuates colinear facilitation in cat primary visual cortex. Experimental Brain Research 143:295-302.
Cudeiro J, Sillito AM (1996) Spatial frequency tuning of orientation-discontinuity-sensitive corticofugal feedback to the cat lateral geniculate nucleus. Journal of Physiology 490:481-492.
Dakin SC, Baruch NJ (2009) Context influences contour integration. Journal of Vision 9:1-13.
Dakin SC, Carlin P, Hemsley D (2005) Weak suppression of visual context in chronic schizophrenia. Current Biology 16:R822-R824.
DeAngelis GC, Freeman RD, Ohzawa I (1994) Length and width tuning of neurons in the cat's primary visual cortex. Journal of Neurophysiology 71:347-374.
Dima D, Dietrich DE, Dillo W, Emrich HM (2010) Impaired top-down processes in schizophrenia: A DCM study of ERPs. NeuroImage 52:824-832.
Dima D, Roiser JP, Dietrich DE, Bonnemann C, Lanfermann H, Emrich HM, Dillo W (2009) Understanding why patients with schizophrenia do not perceive the hollow-mask illusion using dynamic causal modelling. NeuroImage 46:1180-1186.
Duncan RO, Boynton GM (2003) Cortical magnification within human primary visual cortex correlates with acuity thresholds. Neuron 38:659-671.
Engel SA, Glover GH, Wandell BA (1997) Retinotopic organization in human visual cortex and the spatial precision of functional MRI. Cerebral cortex 7:181-192.
Field DJ, Hayes A, Hess RF (1993) Contour integration by the human visual system: Evidence for a local "association field". Vision Research 33:173-193.
First MB (1997) User's guide for the structured clinical interview for DSM-IV axis I disorders SCID-I: clinician version: American Psychiatric Publishing, Inc.
Fletcher PC, Frith CD (2009) Perceiving is believing: A Bayesian approach to explaining the positive symptoms of schizophrenia. Nature Reviews Neuroscience 10:48-58.

Foxe JJ, Murray MM, Javitt DC (2005) Filling-in in schizophrenia: A high-density electrical mapping and source-analysis investigation of illusory contour processing. Cerebral Cortex 15:1914-1927.
Freeman E, Sagi D, Driver J (2001) Lateral interactions between targets and flankers in low-level vision depend on attention to the flankers. Nature Neuroscience 4:1032-1037.
Freeman E, Driver J, Sagi D, Zhaoping L (2003) Top-down modulation of lateral interactions in early vision: Does attention affect integration of the whole or just perception of the parts? Current Biology 13:985-989.
Friston KJ, Holmes AP, Worsley KJ, Poline J-P, Frith CD, Frackowiak RSJ (1994) Statistical parametric maps in functional imaging: A general linear approach. Human Brain Mapping 2:189-210.
Garcia-Perez MA (1998) Forced-choice staircases with fixed step sizes: Asymptotic and small-sample properties. Vision Research 38:1861-1881.
Gilad A, Meirovithz E, Slovin H (2013) Population responses to contour integration: Early encoding of discrete elements and late perceptual grouping. Neuron 78:389-402.
Gilbert C, Ito M, Kapadia M, Westheimer G (2000) Interactions between attention, context and learning in primary visual cortex. Vision Research 40:1217-1226.
Goghari VM, Sponheim SR (2008) Divergent backward masking performance in schizophrenia and bipolar disorder: Association with COMT. American Journal of Medical Genetics Part B 147B:223-227.
Gold JM, Barch DM, Carter CS, Dakin SC, Luck SJ, MacDonald AW, Ragland JD, Ranganath C, Kovacs I, Silverstein SM, Strauss M (2012) Clinical, functional, and intertask correlations of measures developed by the Cognitive Neuroscience Test Reliability and Clinical Applications for Schizophrenia Consortium. Schizophrenia Bulletin 38:144-152.
Gonzalez-Burgos G, Lewis DA (2008) GABA neurons and the mechanisms of network oscillations: Implications for understanding cortical dysfunction in schizophrenia. Schizophrenia Bulletin 34:944-961.
Gooding DC, Grabowski JA, Hendershot CS (2000) Fixation stability in schizophrenia, bipolar, and control subjects. Psychiatry Research 97:119-128.
Green MF, Lee J, Wynn JK, Mathis KI (2011) Visual masking in schizophrenia: Overview and theoretical implications. Schizophrenia Bulletin 37:700-708.
Haider B, Krause MR, Duque A, Yu Y, Touryan J, Mazer JA, McCormick DA (2010) Synaptic and network mechanisms of sparse and reliable visual cortical activity during nonclassical receptive field stimulation. Neuron 65:107-121.
Happé FGE (1996) Studying weak central coherence at low levels: Children with autism do not succumb to visual illusions. A research note. Journal of Child Psychology and Psychiatry 37:873-877.
Hashimoto T, Bazmi HH, Mirnics K, Wu Q, Sampson AR, Lewis DA (2008) Conserved regional patterns of GABA-related transcript expression in the neocortex of subjects with schizophrenia. American Journal of Psychiatry 165:479-489.

Heeger DJ (1992) Normalization of cell responses in cat striate cortex. Visual Neuroscience 9:181-197.
Henry CA, Joshi S, Xing D, Shapley RM, Hawken MJ (2013) Functional characterization of the extraclassical receptive field in macaque V1: Contrast, orientation, and temporal dynamics. The Journal of Neuroscience 33:6230-6242.
Hubel DH, Wiesel TN (1962) Receptive fields, binocular integration and functional architecture in the cat's visual cortex. Journal of Physiology 160:106-154.
Hubel DH, Wiesel TN (1968) Receptive fields and functional architecture of monkey striate cortex. Journal of Physiology 195:215-243.
Huettel SA, Song AW, McCarthy G (2009) Functional magnetic resonance imaging. Sunderland, MA: Sinauer Associates, Inc.
Ichida JM, Schwabe L, Bressloff PC, Angelucci A (2007) Response facillitation from the "suppressive" receptive field surround of macaque V1 neurons. Journal of Neurophysiology 98:2168-2181.
Ishikawa A, Shimegi S, Sato H (2006) Metacontrast masking suggests interaction between visual pathways with different spatial and temporal properties. Vision Research 46:2130-2138.
Ito M, Gilbert CD (1999) Attention modulates contextual influences in the primary visual cortex of alert monkeys. Neuron 22:593-604.
Jahshan C, Wynn JK, McCleery A, Glahn DC, Altshuler LL, Green MF (2014) Cross-diagnostic comparison of visual processing in bipolar disorder and schizophrenia. Journal of Psychiatric Research 51:42-48.
Jeyakumar SLE, Warriner EM, Raval VV, Ahmad SA (2004) Balancing the need for reliability and time efficiency: Short forms of the Wechsler Adult Intelligence Scale-III. Educational and Psychological Measurement 64:71-87.
Joo SJ, Murray SO (2013) Contextual effects in human visual cortex depend on surface structure. In: Vision Sciences Society, p 817. Naples, FL: Journal of Vision.
Joo SJ, Boynton GM, Murray SO (2012) Long-range, pattern-dependent contestual effects in early human visual cortex. Current Biology 22:781-786.
Kastner S, De Weerd P, Desimone R, Ungerleider LG (1998) Mechanisms of directed attention in the human extrastriate cortex as revealed by functional MRI. Science 282:108-111.
Keane B, Silverstein S, Barch D, Carter CS, Gold J, Kovacs I, MacDonald AW, Ragland JD, Strauss ME (2012) The spatial range of contour integration deficits in schizophrenia. Experimental Brain Research 220:251-259.
Keane BP, Joseph J, Silverstein SM (2014) Late, not early, stages of Kanizsa shape perception are compromised in schi. Neuropsychologia 56:301-311.
Keane BP, Silverstein SM, Wang Y, Papathomas TV (2013) Reduced depth inversion illusions in schizophrenia are state-specific and occur for multiple object types and viewing conditions. Journal of Abnormal Psychology 122:506-512.
Kelemen O, Kiss I, Benedek G, Keri S (2013) Perceptual and cognitive effects of antipsychotics in first-episode schizophrenia: The potential imact of GABA

concentration in the visual cortex. Progress in Neuro-Psychopharmacology & Biological Psychiatry 47:13-19.
Kéri DS, Kelemen O, Benedek G (2009) Attentional modulation of perceptual organisation in schizophrenia. Cognitive Neuropsychiatry 14:77-86.
Kéri DS, Kelemen O, Benedek G, Janka Z (2005) Lateral interactions in the visual cortex of patients with schizophrenia and bipolar disorder. Psychological Medicine 35:1043-1051.
Kéri S, Kelemen O, Benedek G, Janka Z (2001) Different trait markers for schizophrenia and bipolar disorder: A neurocognitive approach. Psychological Medicine 31:915-922.
Kingdom FAA, Prins N (2009) Texture-surround suppression of contour-shape coding in human vision. NeuroReport 20:5-8.
Kissler J, Clementz B (1998) Fixation stability among schizophrenia patients. Biological Psychiatry 38:57-62.
Kosovicheva AA, Sheremata SL, Rokem A, Landau AN, Silver MA (2012) Cholinergic enhancement reduces orientation-specific surround suppression but not visual crowding. Frontiers in Behavioral Neuroscience 6:61.
Larsson J (2001) Imaging vision: Functional mapping of intermediate visual processes in man. In: Karolinska Institutet.
Larsson J, Heeger DJ (2006) Two retinotopic visual areas in human lateral occipital cortex. The Journal of Neuroscience 26:13128-13142.
Legge GE (1981) A power law for contrast discrimination. Vision Research 21:457-467.
Legge GE, Foley JM (1980) Contrast masking in human vision. Journal of the Optical Society of America 70:1458-1471.
Levitt JB, Lund JS (1997) Contrast dependence of contextual effects in primate visual cortex. Nature 387:73-76.
Lewis DA, Hashimoto T, Volk DW (2005) Cortical inhibitory neurons and schizophrenia. Nature Reviews Neuroscience 6:312-324.
Li W, Gilbert C (2002) Global contour saliency and local colinear interactions. Journal of Neurophysiology 88:2846-2856.
Li W, Piëch V, Gilbert C (2006) Contour saliency in primary visual cortex. Neuron 50:951-962.
Li W, Piëch V, Gilbert CD (2008a) Learning to link visual contours. Neuron 57:442-451.
Li X, Lu Z-L, Tjan BS, Dosher BA, Chu W (2008b) Blood oxygenation level-dependent contrast response functions identify mechanisms of covert attention in early visual areas. Proceedings of the National Academy of Sciences 105:6202-6207.
Loffler G (2008) Perception of contours and shapes: Low and intermediate stage mechanisms. Vision Research 48:2106-2127.
Lotto RB, Purves D (2001) An empirical explanation of the Chubb illusion. Journal of Cognitive Neuroscience 13:547-555.
Ma W-P, Liu B-H, Li Y-T, Huang ZJ, Zhang LI, Tao HW (2010) Visual representations by cortical somatostatin inibitory neurons - Selective but with weak and delayed responses. The Journal of Neuroscience 30:14371-14379.

McDonald JS, Mannion DJ, Goddard E, Clifford CWG (2010) Orientation-selective chromatic mechanisms in human visual cortex. Journal of Vision 10:34.
Melnick MD, Harrison BR, Park S, Bennetto L, Tadin D (2013) A strong interactive link between sensory discriminations and intelligence. Current Biology 23:1013-1017.
Müller NG, Kleinschmidt A (2004) The attentional'spotlight's' penumbra: center-surround modulation in striate cortex. Neuroreport 15:977-980.
Murray SO (2008) The effects of spatial attention in early human visual cortex are stimulus independent. Journal of Vision 8:2.
Must A, Janka Z, Benedek G, Kéri DS (2004) Reduced facilitation effect of collinear flankers on contrast detection reveals impaired lateral connectivity in the visual cortex of schizophrenia patients. Neuroscience Letters 357:131-134.
Nassi JJ, Lomber SG, Born RT (2013) Corticocortical feedback contributes to surround suppression in V1 of the alert primate. Journal of Neuroscience 33:8504-8517.
Nestares O, Heeger DJ (2000) Robust multiresolution alignment of MRI brain volumes. Magnetic Resonance in Medicine 43:705-715.
Newman EL, Gupta K, Climer JR, Monaghan CK, Hasselmo ME (2012) Cholinergic modulation of cognitive processing: Insights drawn from computational models. Frontiers in Behavioral Neuroscience 6:24.
Nienborg H, Hasenstaub A, Nauhaus I, Taniguchi H, Huang ZJ, Callaway EM (2013) Contrast dependence and differential contributions from somatostatin- and parvalbumin-expressing neurons to spatial integration in mouse V1. The Journal of Neuroscience 33:11145-11154.
Notredame C-E, Pins D, Deneve S, Jardri R (2014) What visual illusions teach us about schizophrenia. Frontiers in Integrative Neuroscience 8:63.
Nurminen L, Angelucci A (2014) Multiple components of surround modulation in primary visual cortex: Multiple neural circuits with multiple functions? Vision Research 104:47-56.
Nurminen L, Kilpelainen M, Laurinen P, Vanni S (2009) Area summation in human visual system: Psychophysics, fMRI, and modeling. Journal of Neurophysiology 102:2900-2909.
Nurnberger JI, Blehar MC, Kaufmann CA, York-Cooler C, Simpson SG, Harkavy-Friedman J, Severe JB, Malaspina D, Reich T (1994) Diagnostic interview for genetic studies: Rationale, unique features, and training. Archives of General Psychiatry 51:849-859.
Olman CA, Yacoub E (2011) High-field fMRI for human applications: An overview of spatial resolution and signal specificity. The Open Neuroimaging Journal 5:74-89.
Olman CA, Inati S, Heeger DJ (2007) The effect of large veins on spatial localization with GE BOLD at 3 T: Displacement, not blurring. NeuroImage 34:1126-1135.
Olman CA, Ugurbil K, Schrater P, Kersten D (2004) BOLD fMRI and psychophysical measurements of contrast response to broadband images. Vision Research 44:669-683.
Overall JE, Donald RG (1962) The brief psychiatric rating scale. Psychological Reports 10:799-812.

Ozeki H, Finn IM, Schaffer ES, Miller KD, Ferster D (2009) Inhibitory stabilization of the cortical network underlies visual surround suppression. Neuron 62:578-592.
Ozeki H, Sadakane O, Akasaki T, Naito T, Shimegi S, Sato H (2004) Relationship between excitation and inhibition underlying size tuning and contextual response modulation in the cat primary visual cortex. The Journal of Neuroscience 24:1428-1438.
Paffen CLE, van der Smagt MJ, te Pas SF, Verstraten FAJ (2005) Center-surround inhibition and facilitation as a function of size and contrast at multiple levels of visual motion processing. Journal of Vision 5:8.
Parnas J, Vianin P, Saebye D, Jansson L, Volmer Larsen A, Bovet P (2001) Visual binding abilities in the initial and advanced stages of schizophrenia. Acta Psychiatrica Scandinavica 103:171-180.
Pelli D (1997) The VideoToolbox software for visual psychophysics: Transforming numbers into movies. Spatial Vision 10:437-442.
Petrov Y, McKee SP (2006) The effect of spatial configuration on surround suppression of contrast sensitivity. Journal of Vision 6.
Phillips WA, Silverstein SM (2013) The coherent organization of mental life depends on mechanisms for context-sensitive gain-control that are impaired in schizophrenia. Frontiers in Psychology 4:307.
Pihlaja M, Henriksson L, James AC, Vanni S (2008) Quantitative multifocal fMRI shows active suppression in human V1. Human Brain Mapping 29:1001-1014.
Place EJS, Gilmore GC (1980) Perceptual organization in schizophrenia. Journal of Abnormal Psychology 89:409-418.
Polat U, Mizobe K, Pettet MW, Kasamatsu T, Norcia AM (1998) Collinear stimuli regulate visual responses depending on cell's contrast threshold. Nature 391:580-584.
Poort J, Raudies F, Wannig A, Lamme VAF, Neumann H, Roelfsema PR (2012) The role of attention in figure-ground segregation in areas V1 and V4 of the visual cortex. Neuron 75:143-156.
Prins N, Kingdom FAA (2009) Palamedes: Matlab routines for analyzing psychophysical In.
Raine A (1991) The SPQ: A scale for the assessment of schizotypal personality based on DSM-III-R criteria. Schizophrenia Bulletin 17:555-564.
Ress D, Backus BT, Heeger DJ (2000) Activity in primary visual cortex predicts performance in a visual detection task. Nature Neuroscience 3:940-945.
Robol V, Casco C, Dakin SC (2012) The role of crowding in contextual influences on contour integration. Journal of Vision 12:1-18.
Robol V, Tibber MS, Anderson EJ, Bobin T, Carlin P, Shergill SS, Dakin SC (2013) Reduced crowding and poor contour detection in schizophrenia are consistent with weak surround inhibition. PLOS ONE 8:e60951.
Roinishvili M, Chkonia E, Brand A, Herzog MH (2008) Contextual suppression and protection in schizophrenic patients. European Archives of Psychiatry and Clinical Neuroscience 258:210-216.

Rokem A, Yoon JH, Ooms RE, Maddock RJ, Minzenberg MJ, Silver MA (2011) Broader visual orientation tuning in patients with schizophrenia. Frontiers in Human Neuroscience 5:127.
Runeson E, Boynton GM, Murray SO (2013) Effects of task and attentional selection on responses in human visual cortex. Journal of Neurophysiology 109:2606-2617.
Sarter M, Hasselmo ME, Bruno JP, Givens B (2005) Unraveling the attentional functions of cortical cholinergic inputs: Interactions between signal-driven and cognitive modulation of signal detection. Brain Research Reviews 48:98-111.
Schallmo M-P, Sponheim SR, Olman CA (2013) Abnormal contextual modulation of visual contour detection in patients with schizophrenia. PLOS ONE 8:e68090.
Schumacher JF, Olman CA (2010) High-resolution BOLD fMRI measurements of local orientation-dependent contextual modulation show a mismatch between predicted V1 output and local BOLD response. Vision Research 50:1214-1224.
Schumacher JF, Thompson SK, Olman CA (2011a) Contrast response functions for single Gabor patches: ROI-based analysis over-represents low-contrast patches for GE BOLD. Frontiers in Systems Neuroscience 5:1-10.
Schumacher JF, Quinn CF, Olman CA (2011b) An exploration of the spatial scale over which orientation-dependent surround effects affect contour detection. Journal of Vision 11:1-12.
Schütze C, Bongard I, Marbach S, Brand A, Herzog MH (2007) Collinear contextual suppression in schizophrenic patients. Psychiatry Research 150:237-243.
Schwartz S, Vuilleumier P, Hutton C, Maravita A, Dolan RJ, Driver J (2005) Attentional load and sensory competition in human vision: Modulation of fMRI responses by load at fixation during task-irrelevant stimulation in the peripheral visual field. Cerebral Cortex 15:770-786.
Seymour K, Stein T, Sanders LLO, Guggenmos M, Theophil I, Sterzer P (2013) Altered contextual modulation of primary visual cortex responses in schizophrenia. Neuropsychopharmacology 38:2607-2612.
Shmuel A, Yacoub E, Pfeuffer J, Van de Moortele P-F, Adriany G, Hu X, Ugurbil K (2002) Sustained negative BOLD, blood flow and oxygen consumption response and its coupling to the positive response in the human brain. Neuron 36:1195-1210.
Shushruth S, Mangapathy P, Ichida JM, Bressloff PC, Schwabe L, Angelucci A (2012) Strong recrrent networks compute the orientation tuning of surround modulation in the primate primary visual cortex. The Journal of Neuroscience 32:308-321.
Shushruth S, Nurminen L, Bijanzadeh M, Ichida JM, Vanni S, Angelucci A (2013) Different orientation tuning of near- and far-surround suppression in macaque primary visual cortex mirrors their tuning in human perception. The Journal of Neuroscience 33:106-119.
Silver MA, Ress D, Heeger DJ (2007) Neural correlates of sustained spatial attention in human early visual cortex. Journal of Neurophysiology 97:229-237.

Silverstein S, Keane B (2011) Perceptual organization impairment in schizophrenia and associated brain mechanisms: Review of research from 2005 to 2010. Schizophrenia Bulletin 37:690-699.
Silverstein S, Uhlhaas P, Essex B, Halpin S, Schall U, Carr V (2006a) Perceptual organization in first episode schizophrenia and ultra-high-risk states. Schizophrenia Research 83:41-52.
Silverstein S, Berten S, Essex B, Kovacs I, Susmaras T, Little DM (2009) An fMRI examination of visual integration in schizophrenia. Journal of Integrative Neuroscience 8:175-202.
Silverstein S, Keane B, Barch D, Carter CS, Gold J, Kovacs I, MacDonald AW, Ragland JD, Strauss ME (2012) Optimization and validation of a visual integration test for schizophrenia research. Schizophrenia Bulletin 38:125-134.
Silverstein S, Hatashita-Wong M, Schenkel L, Wilkniss S, Kovacs I, Feher A, Smith T, Goicochea C, Uhlhaas P, Carpiniello K, others (2006b) Reduced top-down influences in contour detection in schizophrenia. Cognitive Neuropsychiatry 11:112-132.
Silverstein SM, Kovacs I, Corry R, Valone C (2000) Perceptual organization, the disorganization syndrome, and context processing in chronic schizophrenia. Schizophrenia Research 43:11-20.
Skottun BC, Skoyles JR (2007) Contrast sensitivity and magnocellular functioning in schizophrenia. Vision Research 47:2923-2933.
Smith AT, Williams AL, Singh KD (2004a) Negative BOLD in the visual cortex: Evidence against blood stealing. Human Brain Mapping 21:213-220.
Smith AT, Singh KD, Williams AL, Greenlee MW (2001) Estimating receptive field size from fMRI data in human striate and extrastriate visual cortex. Cerebral Cortex 11:1182-1190.
Smith SM, Jenkinson M, Woolrich MW, Beckmann CF, Behrens TEJ, Johansen-Berg H, Bannister PR, De Luca M, Drobnjak I, Flitney DE, Niazy R, Saunders J, Vickers J, Zhang Y, De Stefano N, Brady JM, Matthews PM (2004b) Advances in functional and structural MR image analysis and implementation as FSL. NeuroImage 23:208-219.
Snowden RJ, Hammett ST (1998) The effects of surround contrast on contrast thresholds, perceived contrast, and contrast discrimination. Vision Research 38:1935-1945.
Solomon SG, White AJR, Martin PR (2002) Extraclassical receptive field properties of parvocellular, magnocellular, and koniocellular cells in the primate lateral geniculate nucleus. The Journal of Neuroscience 22:338-349.
Spencer KM, Nestor PG, Niznikiewicz MA, Salisbury DF, Shenton ME, McCarley RW (2003) Abnormal neural synchrony in schizophrenia. The Journal of Neuroscience 23:7404-7411.
Spencer KM, Nestor PG, Perlmutter R, Niznikiewicz MA, Klump MC, Frumin M, Shenton ME, McCarley RW (2004) Neural synchrony indexes disordered perception and cognition in schizophrenia. Proceedings of the National Academy of Sciences 101:17288-17293.

Sponheim SR, Sass SM, Noukki AL, Hegeman BM (2012) Fragile early visual percepts mark genetic liability specific to schizophrenia. Schizophrenia Bulletin.
Tadin D, Kim J, Doop ML, Gibson C, Lappin JS, Blake R, Park S (2006) Weakened center-surround interactions in visual motion processing in schizophrenia. The Journal of Neuroscience 24:11403-11412.
Tibber MS, Anderson EJ, Bobin T, Antonova E, Seabright A, Wright B, Carlin P, Shergill S, Dakin SC (2013) Visual surround suppression in schizophrenia. Frontiers in Psychology 4:1-13.
Tootell RBH, Hadjikhani N, Hall EK, Marrett S, Vanduffel W, Vaughan JT, Dale AM (1998) The retinotopy of visual spatial attention. Neuron 21:1409-1422.
Uhlhaas PJ, Phillips WA, Silverstein SM (2005) The course and clinical correlates of dysfunctions in visual perceptual organization in schizophrenia during the remission of psychotic symptoms. Schizophrenia Research 75:183-192.
Uhlhaas PJ, Silverstein SM, Phillips WA, Lovell PG (2004) Evidence for impaired visual context processing in schizotypy with thought disorder. Schizophrenia Research 68:249-260.
Uhlhaas PJ, Phillips WA, Mitchell G, Silverstein SM (2006) Perceptual grouping in disorganized schizophrenia. Psychiatry Research 145:105-117.
Walker GA, Ohzawa I, Freeman RD (1999) Asymmetric suppression outsize the classical receptive field of the visual cortex. The Journal of Neuroscience 19:10536-10553.
Walter E, Dassonville P, Bochsler TM (2009) A specific autistic trait that modulates visuospatial illusion susceptibility. Journal of Autism and Developmental Disorders 39:339-349.
Webb BS, Dhruv NT, Solomon SG, Tailby C, Lennie P (2005) Early and late mechanisms of surround suppression in striate cortex of macaque. The Journal of Neuroscience 25:11666-11675.
Wertheimer M (1938) Laws of organization in perceptual forms. In: A source book of Gestalt psychology (Ellis WD, ed), pp 71-88. London: Kegan Paul, Trench, Trubner & Company.
Williams AL, Singh KD, Smith AT (2003) Surround modulation measured with functional MRI in the human visual cortex. Journal of Neurophysiology 89:525-533.
Wilson S, Sponheim SR (2014) Dimensions underlying psychotic and manic symptomatology: Extending normal-range personality traits to schizophrenia and bipolar spectra. Comprehensive Psychiatry 55:1809-1819.
Xing J, Heeger DJ (2000) Center-surround interactions in foveal and peripheral vision. Vision Research 40:3065-3072.
Xu W-F, Shen Z-M, Li C-Y (2005) Spatial phase sensitivity of V1 neurons in alert monkey. Cerebral Cortex 15:1697-1702.
Yang E, Tadin D, Glasser DM, Hong SW, Blake R, Park S (2013) Visual context processing in schizophrenia. Clinical Psychological Science 1:5-15.

Yoon JH, Sheremata SL, Rokem A, Silver MA (2013) Windows to the soul: Vision science as a tool for studying biological mechanisms of information processing deficits in schizophrenia. Frontiers in Psychology 4:681.
Yoon JH, Rokem AS, Silver MA, Minzenberg MJ, Ursu S, Ragland JD, Carter CS (2009) Diminished orientation-specific surround suppression of visual processing in schizophrenia. Schizophrenia Bulletin 35:1078-1084.
Yoon JH, Maddock RJ, Rokem A, Silver MA, Minzenberg MJ, Ragland JD, Carter CS (2010) GABA concentration is reduced in visual cortex in schizophrenia and correlates with orientation-specific surround suppression. The Journal of Neuroscience 30:3777-3781.
Yu C, Klein SA, Levi DM (2001) Surround modulation of perceived contrast and the role of brightness induction. Journal of Vision 1:18-31.
Yu C, Klein SA, Levi DM (2003) Cross-and iso-oriented surrounds modulate the contrast response function: The effect of surround contrast. Journal of Vision 3.
Zeng C, Li Y, Li C (2011) Center-surround interaction with adaptive inhibition: A computational model for contour detection. NeuroImage 55:49-66.
Zenger-Landolt B, Koch C (2001) Flanker effects in peripheral contrast discrimination - psychophysics and modeling. Vision Research 41:3663-3675.
Zenger-Landolt B, Heeger DJ (2003) Response suppression in V1 agrees with psychophysics of surround masking. The Journal of Neuroscience 23:6884-6893.
Zenger B, Braun J, Koch C (2000) Attentional effects on contrast detection in the presence of surround masks. Vision research 40:3717-3724.